DOKUZ EYLÜL UNIVERSITY
GRADUATE SCHOOL OF NATURAL AND APPLIED SCIENCES

MAGNETIC PROPERTIES OF THE SPIN-1 BLUME-EMERY-GRIFFITHS MODEL IN THE PRESENCE OF MAGNETIC FIELD

by
Yusuf YÜKSEL

July, 2008
İZMİR

MAGNETIC PROPERTIES OF THE SPIN-1 BLUME-EMERY-GRIFFITHS MODEL IN THE PRESENCE OF MAGNETIC FIELD

A Thesis Submitted to the
Graduate School of Natural and Applied Sciences of
Dokuz Eylül University
In Partial Fulfillment of the Requirements for
the Degree of Master of Science in Physics

by
Yusuf YÜKSEL

July, 2008
İZMİR

M.Sc THESIS EXAMINATION RESULT FORM

We have read the thesis entitled "**MAGNETIC PROPERTIES OF THE SPIN-1 BLUME-EMERY-GRIFFITHS MODEL IN THE PRESENCE OF MAGNETIC FIELD**" completed by **YUSUF YÜKSEL** under supervision of **PROF. DR. HAMZA POLAT** and we certify that in our opinion it is fully adequate, in scope and in quality, as a thesis for the degree of Master of Science.

.....
Prof. Dr. Hamza POLAT

Supervisor

.....	.....
Prof. Dr. Kadir YURDAKOÇ	Assoc. Prof. Dr. Cesur EKİZ
(Jury Member)	(Jury Member)

Prof. Dr. Cahit HELVACI
Director
Graduate School of Natural and Applied Sciences

ACKNOWLEDGMENTS

I am deeply indebted to my supervisor, Prof. Dr. Hamza POLAT for his encouragement, guidance and support. I would like to thank Assoc. Prof. Dr. Ekrem AYDINER whose help and stimulating suggestions helped me in all the time of research. I would also like to thank Ümit AKINCI for his precious suggestions and discussions. I am deeply grateful to him. Particular thanks are due to Cenk AKYÜZ, Aytaç Gürhan GÖKÇE and Sevil SARIKURT for their helpful comments on the LaTeX codes of manuscript.

Especially, I would like to give my all special thanks and gratitude to my family whose patient love enabled me to complete this work.

This work has been supported by TÜBİTAK (Scientific and Technical Research Council of Turkey) with 24 months Master of Science Grant Program (Code Number: 2210).

Yusuf YÜKSEL

MAGNETIC PROPERTIES OF THE SPIN-1 BLUME-EMERY-GRIFFITHS MODEL IN THE PRESENCE OF MAGNETIC FIELD

ABSTRACT

Magnetic properties of the spin-1 Blume-Capel (BC) model and Blume-Emery-Griffiths (BEG) model on square lattice are presented within the framework of the effective-field theory (EFT) with correlations approximation method and Monte Carlo simulation technique. We have improved the EFT method by including the correlations between different spins which emerge when expanding the identities. In order to do this, we have derived a set of linear equations for the considered systems by taking as a basis the thermal averages of a central spin and a perimeter spin at the site i, which is defined within the spin identities and differential operator technique. By solving numerically the set of linear equations derived for the Ising system with coordination number q=4, we have evaluated all the spin correlation functions without using any kind of decoupling approximation in the spin system under a longitudinal magnetic field. The effects of the longitudinal magnetic field on magnetic properties of the spin systems are discussed in detail. Numerical computations are performed and the results are analyzed for the cases of the spin-1 BC model by using effective-field theory with correlations and spin-1 BEG model by applying Monte Carlo simulations on the square lattice, respectively. We have also evaluated the phase diagrams for the spin-1 BC model on square lattice.

Keywords: I-EFT approximation, MC simulation, spin-1 Ising model, square lattice.

DIŞ MAGNETİK ALANIN VARLIĞINDAKİ SPİN-1 BLUME-EMERY-GRIFFITHS MODELİN MAGNETİK ÖZELLİKLERİ

ÖZ

Bu çalışmada, korelasyonlu efektif alan teorisi ve Monte Carlo simülasyon tekniği temel alınarak kare örgüde spin-1 Blume-Capel (BC) ve Blume-Emery-Griffiths (BEG) modelin manyetik özellikleri incelendi. Geliştirdiğimiz efektif alan teorisinde, spin özdeşlikleri ve diferansiyel operotör tekniği ile tanımlanmış, i konumunda bulunan komşu spinlerin ve merkezi spinin termal ortalamaları temel alınarak, lineer eşitlikler kümesi elde edildi. Bu amaçla, en yakın komşu sayısı q=4 olan spin-1 Blume-Capel modeli için türetilmiş olan lineer eşitlikler kümesi sayısal olarak çözülerek, dış manyetik alan altındaki spin sisteminde herhangi bir eşleme yaklaşımı kullanılmadan bütün korelasyon fonksiyonları numerik olarak hesaplandı. Boyuna manyetik alanın, kristal alan teriminin ve bikuadratik değiş-tokuş etkileşme teriminin, söz konusu sistemlerin manyetik özellikleri üzerindeki etkileri ayrıntılı olarak tartışıldı. Sırasıyla, efektif alan teorisi temel alınarak BC model, Monte Carlo simülasyon tekniği kullanılarak ise BEG model için kare örgüde nümerik hesaplamalar yapıldı ve sonuçlar analiz edildi. Ayrıca, kare örgüde spin-1 BC model için faz diyagramları ele alındı.

Anahtar sözcükler: I-EFT yaklaşımı, MC simülasyonu, spin-1 Ising modeli, kare örgü.

CONTENTS

CHAPTER ONE
INTRODUCTION

1.1 Introduction

The Ising model has been one of the most actively studied systems in statistical mechanics and has been used as an elementary model to describe the phenomena of phase transition for cooperative physical systems. The reason is due to the fact that they can describe fairly well numerous physical systems, such as magnetic spin systems, binary alloys, lattice gas, and so on.

The simplest form of the Ising model appears in one-dimensional lattice (linear chain) consisting of spin-1/2 atoms, with nearest-neighbor interactions and in the absence of an external field. It was in this form that Ising proposed his model in 1925, in order to study the magnetic phase transition. However, he did not find a long-range order at any finite temperature. Indeed, one may say that the Ising chain undergoes a phase transition at zero temperature.

However, the two dimensional (square lattice) Ising model in the absence of an external field does show a phase transition at a finite temperature, which was solved exactly by Onsager in 1944 (Onsager, 1944). After Onsager's solution, the Ising model has been one of the most actively studied problems in statistical mechanics. Some rigorous solutions have been given for the simple Ising model with S=1/2 on one-dimensional and certain two-dimensional lattices.

In the other case, the model must be solved by approximation method or numerical method, such as the molecular field approximation (MFA), the Bethe-Peierls approximation (B-PA) (Bethe, 1935; Peierls, 1936), the Bethe lattice approximation (BLA) (Tanaka & Uryu, 1981), in which the lattice is simplified as an infinite Cayley tree with the coordination number z, the effective field theory (EFT) (Kaneyoshi et al, 1981; Honmura & Kaneyoshi, 1979; Kaneyoshi et

al, 1992b; Siqueira & Fittipaldi, 1986), the double-chain approximation (DCA) (Yokota, 1988), which is a natural extension of the pair approximation, the cluster variation method (CVM) (Micnas, 1979; Ng & Barry, 1978), the series expansion method (SE) which is valid for temperatures either very high or very low compared with the transition temperature (Baxter, 1982; Saul et al, 1974), the Monte Carlo technique (MC) (Pawley et al, 1984; Rachadi & Benyoussef, 2004), and so on.

The transition temperatures obtained by the former seven approximation methods are higher than the exact value, the B-PA and BLA give the same transition temperatures for $S = 1/2$, and the DCA with the large cluster gives the transition temperature closing mostly to the exact value. There are also many results based on the renormalization-group methods, especially for the critical region of the model.

The EFT is based on the identities valid for Ising systems, using the differential operator technique, it converts the problem of calculation of the trace for spin operator to calculation of the derivative of a given function. Therefore the relation between the expectation value of a given spin and the multi-spin correlation functions composed of its neighbor spins is obtained. Adopting the Zernike approximation to decompose the multi-spin correlation function to the multiplication of the single spin correlation functions, thus the magnetization of the system can be calculated. Essentially, the EFT is a cluster method in which the central spin and its neighbor spins are considered.

Because of the smaller cluster taken in the approximation, the results obtained by the EFT are not too accurate. For example, the transition temperature k_BT_c/J (where J is the exchange interaction between the nearest-neighbor spins) obtained by EFT is 0.773 for $S = 1/2$ Ising model on the square lattice, and the exact result is 0.567, the difference is apparent. By considering the fluctuation of spins in decoupling of the multi-spin correlation function, the correlated effective field theory (CEFT) improves the results, and gets 0.721 (Kaneyoshi et al, 1981; Honmura & Kaneyoshi, 1979; Kaneyoshi et al, 1992b; Siqueira & Fittipaldi, 1986; Kaneyoshi & Tamura, 1982).

Further improvement of the decoupling approximation to the multi-spin correlation function, called DA (Kaneyoshi, 2000), the result becomes 0.686. The dimensionality of the system can not be distinguished in EFT approximation.

B-PA is also a cluster method (Bethe, 1935; Peierls, 1936), in which the central spin and its neighbor spins are taken as a cluster, and the neighboring spins are in an effective field produced by the other spins outside the cluster. The effective field is determined by the condition that the expectation value of the central spin is equal to that of the neighboring spins. From the point of view of the cluster taken in the EFT and B-PA, the two methods are equal in approximation. It is indeed proved that the CEFT is equivalent to B-PA in accuracy in calculation of the transition temperature of system for $S = 1/2$ (Kaneyoshi et al, 1981; Honmura & Kaneyoshi, 1979; Kaneyoshi et al, 1992b; Siqueira & Fittipaldi, 1986; Kaneyoshi & Tamura, 1982). In addition, the B-PA approximation becomes exact on the Bethe lattice (BLA) for $S = 1/2$ (Tanaka & Uryu, 1981), so the B-PA has been applied to many areas for its clear physics idea and simple calculation, although it can not distinguish the dimensionality of the system, too.

Because of its simplicity, the molecular-field approximation (MFA) has played an important role for the description of cooperative phenomena since the concept of the molecular field was introduced by Weiss in a phenomenological model for ferromagnetism. The theory can be relied on for an appropriate description of the major aspects of the phenomena being studied. However, the MFA has some deficiencies, due to the neglect of correlations when MFA results are compared with experiments. Improvements in this aspect have been sought by many methods.

Moreover, like the EFT and B-PA, the MFA can not distinguish the dimensionality of lattice, the formulae derived depend only on the coordination number z, so the square lattice ($z = 4$) and kagomé lattice ($z = 4$) is same in these approximation methods , and so are the two-dimensional triangular lattice ($z = 6$) and the three-dimensional simple cubic lattice ($z = 6$).

On the other hand, in the expanded Bethe-Peierls approximation, the system is taken as a group of chains composed of a central chain and its nearest-neighbor chains. The nearest-neighbor chains are in an effective field produced by the other spins, which can be determined by the condition that the magnetization of the central chain is equal to that of its nearest-neighbor chains. Unlike the case in MFA, EFT and B-PA, the lattice dimensionality depends only on the coordination numbers, the three-dimensional simple cubic (SC) lattice ($z = 6$) and the two-dimensional triangular (TRI) lattice ($z = 6$) cannot be distinguished, in the expanded Bethe-Peierls approximation, the lattice dimensionality of the system can be distinguished in the formulations, so it can be used to study the difference of the properties of the systems on SC and TRI lattices.

The aim of our work is to study the effects of crystal field interaction on the magnetic properties of the spin systems in a magnetic field with (or without) biquadratic exchange interaction by applying MC simulations and using the introduced EFT approximation. The main difference of our introduced EFT approximation used in this study, in comparison with any decoupling approximation can be seen in the expanding of the right hand side of the equations for thermal averages of the central spin and the perimeter spin, respectively.

In the absence of a longitudinal magnetic field, we have discussed the order parameter magnetization, susceptibility, internal energy, specific heat and have investigated the phase diagrams of spin-1 Ising ferromagnetic system with the coordination number $q = 4$ by applying Monte Carlo simulation technique and introduced EFT approximation without using any kind of decoupling approximation (DA) in the spin system with crystal field and biquadratic exchange interaction (Polat et al, 2003).

It was found that the critical phase transition temperatures of spin-1 system with crystal field and biquadratic exchange interaction obtained by using EFT approximation are lower than those obtained by EFT in the literature, while the results of our MC simulations are agree with those obtained by (Adler & Enting,

1984; Fox & Guttman, 1973; Blote & Nightingale, 1985; Saul et al, 1974).

As far as we know, there are a few works for spin-1 system with crystal field in a longitudinal external field and less attention has been given to calculate the hysteresis loop, susceptibility, internal energy and specific heat, owing to mathematical complexities. Therefore we want to study the spin-1 Ising model on square lattice in the presence of a longitudinal magnetic field with the use of MC simulations and introduced EFT approximation, in which the correlations between different spins which emerge when expanding the identities are included. This method is an alternative derivation of the Bethe-Peierls approximation (BPA) (Bethe, 1935; Peierls, 1936), namely the $(q+1)$ site cluster theory (CT) with a central site and the q nearest-neighbor sites, within the differential operator technique in the Ising models (Kaneyoshi, 1992).

CHAPTER TWO
SPIN SYSTEMS

The aim of this chapter is to describe some of the most fundamental models of cooperative behavior. To model a physical system one route is to include, as realistically as possible, all the complicated many body interactions and try to obtain a quantitative prediction of the behavior by solving Schrodinger's equation numerically. The other extreme is to write down the simplest possible model that still includes the essential physics and hope that it is tractable to analytic or precise numerical solution. The aim here is often to study universal behavior or to gain a qualitative understanding of the physics governing the behavior of a given class of materials. It is the latter approach that we shall take here. Despite the apparent simplicity of the models, they show a rich mathematical structure and are in general difficult or, more usually, impossible to solve exactly. Moreover, and perhaps surprisingly at first sight, they do provide valid and useful representations of experimental systems. It is conventional and convenient to use magnetic language and write the model Hamiltonians in terms of spin variables, although they will turn out to be applicable to many non-magnetic systems. In all the examples considered here the spins will lie on the sites i of a regular lattice. Three-dimensional lattices, such as simple cubic, body-centered cubic, and face-centered cubic, are familiar from conventional crystallography but we shall also be interested in lattices in two dimensions.

2.1 Spin-1/2 Ising Model

Spin-1/2 Ising model was firstly introduced by Lenz (1920), and was later on worked out in detail by his pupil Ising (1925). Originally, it was invented for the phase transition of ferromagnets at the Curie temperature; however, in the course of its time it was realized that with only slight changes the model can also be

applied to other phase transitions, like order-disorder phase transitions in binary alloys. Furthermore, the model may be applied to several modern problems of many particle physics, for instance for the description of so-called spin glasses. These are metals having amorphous instead of crystalline structures, which have the interesting property of non-vanishing entropy at $T = 0$. Recently, it has been realized that Ising's idea (in modified form) could also explain pattern recognition in schematic neural networks. Thus, this model gains more and more importance for the development of models for the human brain.

The simplest form for the Hamiltonian of the spin-1/2 Ising model can be written as

$$H = -J \sum_{<ij>} S_i S_j - h \sum_i S_i$$

where $S_i = \pm 1/2$. $J > 0$ corresponds to ferromagnetic case while $J < 0$ corresponds to antiferromagnetic case.

Ising studied the simplest possible model consisting simply of a linear chain of spins, and showed that for this one-dimensional case there is no (non-zero) critical temperature (i.e., the spins become aligned only at $T = 0$). Ten years elapsed before Peierls showed that the two-dimensional model does have a non-zero spontaneous magnetization, and can therefore be regarded as a valid model of a ferromagnet.

In 1944, the physicist Lars Onsager, studying the two-dimensional Ising model on a square lattice, was able to demonstrate by analytical means the existence of a phase transition in the model, a result considered to be a landmark in the physics of critical phenomena, (Yeomans, 2000).

2.2 Spin-1 Ising Model

In addition to spin-1/2 Ising model, spin-1 Ising models are also encountered in different fields of physics and continue to be one of the most actively studied problems in statistical mechanics. For example, the most general Hamiltonian for the spin-1 Ising model is

$$H = -J \sum_{<ij>} S_i S_j - D \sum_i S_i^2 - K \sum_{<ij>} S_i^2 S_j^2 - L \sum_{<ij>} \left(S_i^2 S_j + S_i S_j^2 \right) - h \sum_i S_i \tag{2.2.1}$$

where $S_i = \pm 1, 0$. This follows from allowing all possible terms $S_i^\alpha S_j^\beta$; $\alpha, \beta = 0, 1, 2$. Higher powers of the spin do not enter because $S_i^3 = S_i$.

In contrast to the spin-1/2 Ising model, they are of particular importance, because of the fundamental interest in the multi-critical phenomena of physical systems, such as ^{3}He $-^4$ He mixtures, ternary alloys, meta-magnets and multi-component fluids. In particular, the spin-1 Ising model with a crystal field interaction is often called the Blume-Capel (BC) model (Capel, 1966; Blume, 1966) and the Blume-Emery-Griffiths (BEG) model (Blume & Emery & Griffiths, 1971) contains a biquadratic exchange interaction and a single ion anisotropy in addition to the bilinear exchange interaction.

2.3 The q-State Potts Model

Many different spin models, some driven by theoretical and some by experimental considerations, have been defined in the scientific literature. The only other classical spin model that we shall define here is the q-state Potts model. The relation of this system to the physisorption of krypton atoms on a graphite surface provides an interesting example of how to construct a model Hamiltonian with the correct symmetry.

To define the Potts model a q-state variable, $\alpha_i = 1, 2, 3, ..., q$, is placed on each

lattice site. The interaction between the spins is described by the Hamiltonian

$$H = -J \sum_{<ij>} \delta_{\alpha_i \alpha_j} \tag{2.3.1}$$

δ is a Kronecker delta-function so the energy of two neighboring spins is $-J$ if they lie in the same state and zero otherwise. It is easy to convince oneself that the Potts model has q equivalent ground states where all the spins are identical but can take any one of the q values. As the temperature is increased there is a transition to a paramagnetic phase which is continuous for $q \leq 4$ but first-order for $q > 4$ in two dimensions.

For $q = 2$, the Potts model is identical to the spin-1/2 Ising model. Note, however, that for $q = 3$ the Hamiltonian (2.3.1) does not correspond to the first term in equation (2.2.1) because the three states of the spin-1 Ising model are not equivalent, (Yeomans, 2000).

2.4 Heisenberg Model

The restriction of the Ising model is that the spin vector can only lie parallel to the direction of quantization introduced by the magnetic field. This means that the Ising Hamiltonian can only prove useful in describing a magnet which is highly anisotropic in spin space. There are physical systems, MnF_2 for example, which to a good approximation obey this criterion, but fluctuations of the spin away from the axis of quantization must inevitably occur to some degree.

A more realistic model of many magnets with localized moments is

$$H = -J_z \sum_{<ij>} S_i^z S_j^z - J_\perp \sum_{<ij>} (S_i^x S_j^x + S_i^y S_j^y) - h \sum_i S_i^z \tag{2.4.1}$$

where x, y and z labels are Cartesian axes in spin space. For $J_\perp = J_z$ (2.4.1) can

be written

$$H = -J \sum_{<ij>} \overrightarrow{S_i}.\overrightarrow{S_j} - h \sum_i S_i^z \tag{2.4.2}$$

This is the Heisenberg model.

The Heisenberg model was introduced in 1928 and was discussed in some detail as a model of ferromagnetism. It gives a reasonable description of the properties of some magnetic insulators, such as EuS, and provides a microscopic Hamiltonian describing the exchange interaction which leads to ferromagnetism. However, it does not include the possibility of non-localized spins and assumes complete isotropy in spin space. The most fundamental theoretical difference between the Heisenberg and Ising models is that for the former the spin operators do not commute. Therefore it is a quantum mechanical rather than a classical spin model with corresponding greater difficulty in analytic or numerical treatments.

Quantum models can be mapped on to classical spin systems in one higher dimension and there are some exact results for one-dimensional quantum models, just as for two-dimensional classical models. Moreover, just as the Ising model only has a finite temperature phase transition for $d > 1$, the Heisenberg model orders at zero temperature unless $d > 2$. The classical limit of the Heisenberg model can be constructed by taking the number of spin components to infinity and normalizing the spin from $\sqrt{S(S+1)}$ to 1. The spins become three-dimensional classical vectors. This limit, which leads to considerable simplifications in theoretical work, is useful because the critical exponents of the classical and quantum Heisenberg models are the same. This is an example of universality, (Yeomans, 2000).

2.5 XY Model

A second quantum mechanical spin model is the X-Y model, equation (2.4.1) obtained by putting $J_z = 0$ in the Hamiltonian

$$H = -J_\perp \sum_{<ij>} (S_i^x S_j^x + S_i^y S_j^y) - h_x \sum_i S_i^x \tag{2.5.1}$$

This leads to spins which are two-dimensional, quantum mechanical vectors. The X-Y model, like the Heisenberg model, only has a conventional phase transition at non-zero temperature for $d > 2$. However, in $d = 2$ there is a transition at finite temperatures to an unusual ordered phase with quasi long-range order. This is marked by the correlations decaying algebraically for all temperatures, not just at the critical point itself.

CHAPTER THREE
EFFECTIVE FIELD THEORY

3.1 Callen Identity and Differential Operator Technique

The Ising model of ferromagnetism is a model whereby, because of an extreme field of anisotropy, only the z component of a spin exists. The Hamiltonian of the model, in an external field h, is given by

$$H = -\frac{1}{2}\sum_{i,j} J_{ij}\mu_i\mu_j - h\sum_i \mu_i \tag{3.1.1}$$

where the sums run N identical spins. μ_i is the dynamical variable which can take two values, ± 1, and J_{ij} the exchange interaction between a site i and a site j. That is to say, μ_i is the z component of a spin operator ($S_i^z = (1/2)\mu_i$) associated with the ion localized at the site i which can take spin up ($\mu_i = +1$) or down ($\mu_i = -1$). The spin system is ordered when all spins are up (or down) in a ferromagnet ($J_{ij} > 0$). The magnetic field is added in order to break the symmetry and favor the ordered phase to be up or down. The parameter that measures the ordering of the system (or the long-range order parameter) is given by $m = \langle \mu_i \rangle$. In the ordered phase $m \neq 0$, while in the disordered phase $m = 0$.

The expectation value of the spin variable at the site i is given by

$$\langle m_i \rangle = \frac{1}{Z}\mathrm{Tr}\mu_i e^{-\beta H} \tag{3.1.2}$$

with

$$Z = \mathrm{Tr}e^{-\beta H} \tag{3.1.3}$$

where Tr means the sum over allowed states of the system. Here, $\beta = 1/k_B T$, where k_B is the Boltzmann constant and T is the absolute temperature.

We know now that an exact relation can be derived for the expectation value

(3.1.2), when the Hamiltonian is given by (3.1.1). For the derivation, let us separate the Hamiltonian (3.1.1) into two parts; one (denoted by H_i) which includes all contribution associated with the site i, and the other (denoted by $H^{'}$) which does not depend on the site i. Then, one has

$$H = H_i + H^{'} \tag{3.1.4}$$

with

$$H_i = -\mu_i E_i \tag{3.1.5}$$

and

$$E_i = \sum_{i,j} J_{ij}\mu_j + H \tag{3.1.6}$$

where E_i is the operator expressing the local field on the site i. Here, notice that the spin variables commute, i.e. $[\mu_i, \mu_j] = 0$, and hence

$$[H_i, H^{'}] = [H_i, H] = 0 \tag{3.1.7}$$

in the Ising model.

Because of the commutative relation, the expectation value (3.1.2) can be expressed as

$$\langle \mu_i \rangle = \frac{1}{Z}\left\{ \mathrm{Tr} e^{-\beta H}\left[\frac{\mathrm{tr}\mu_i \exp\left(-\beta H_i\right)}{\mathrm{tr}\exp\left(-\beta H_i\right)} \right] \right\} \tag{3.1.8}$$

where $\mathrm{tr}_{(i)} = \sum_{\mu_i=-1}^{+1}$ stands for the trace associated with the variable at the site i. By doing the partial trace of μ_i, one obtains

$$\langle \mu_i \rangle = \frac{1}{Z}\mathrm{Tr}\left[e^{-\beta H}\tanh(\beta E_i) \right] \tag{3.1.9}$$

or

$$\langle \mu_i \rangle = \langle \tanh(\beta E_i) \rangle$$

This is the identity first derived by Callen in 1963 (Callen, 1963). By extending the above procedure, the identity can be easily generalized to

$$\langle \{f_i\}\mu_i \rangle = \langle \{f_i\}\tanh(\beta E_i) \rangle \tag{3.1.10}$$

where $\{f_i\}$ can take any function of the Ising variables as long as it is not a function of the site i.

Furthermore, the above derivation of (3.1.9) can be also generalized to the Ising model with a general spin S expressed by

$$H = -\frac{1}{2}\sum_{i,j} J_{ij} S_i^z S_j^z - h\sum_i S_i^z \tag{3.1.11}$$

where S_i^z takes the $(2S+1)$ components allowed for a spin value S. Then, one obtains

$$\langle\{f_i\}S_i^z\rangle = S\langle\{f_i\}B_s(\beta E_i)\rangle \tag{3.1.12}$$

with

$$E_i = \sum J_{ij} S_j^z + H \tag{3.1.13}$$

where $B_s(x)$ is the Brillouin function (Suzuki, 1965).

At this place, notice that the standard mean field theory can be obtained from (3.1.9) or (3.1.12) by approximating the thermal average of the hyperbolic tangent (or the Brillouin function) with the thermal average of E_i, i.e.,

$$\langle\tanh(\beta E_i)\rangle \approx \tanh(\beta\langle E_i\rangle) \tag{3.1.14}$$

or

$$\langle B_s(\beta E_i)\rangle \approx B_s(\beta\langle E_i\rangle)$$

Thus, the exact identities (3.1.9), (3.1.10) and (3.1.12) give a way to improve the mean field approximation.

First approach to Callen identity was introduced by Matsudai (Matsudaira, 1973). In order to treat the Callen identity (3.1.9), he noticed the following exact relations which are valid for $\mu = \pm 1$.

$$\tanh(K\mu_1) = A\mu_1, \qquad A = \tanh K, \qquad \tanh[K(\mu_1+\mu_2)] = B(\mu_1+\mu_2)$$

$$B = \frac{1}{2}\tanh 2K, \qquad \tanh[K(\mu_1+\mu_2+\mu_3)] = C_1(\mu_1+\mu_2+\mu_3) + C_2\mu_1\mu_2\mu_3$$

$$C_1 = \frac{1}{4}(\tanh 3K + \tanh K), \qquad C_2 = \frac{1}{4}(\tanh 3K - \tanh K) \tag{3.1.15}$$

and so on, where $K = \beta J$ for nearest-neighbor interaction J. For instance, the identity (3.1.9) for the honeycomb lattice with coordination number $q = 3$ can be, upon using the exact relation (3.1.15), rewritten as

$$\langle \mu_i \rangle = C_1 \left(\langle \mu_{i+1} \rangle + \langle \mu_{i+2} \rangle + \langle \mu_{i+3} \rangle \right) + C_2 \langle \mu_{i+1}\mu_{i+2}\mu_{i+3} \rangle \tag{3.1.16}$$

where $i + \delta$ ($\delta = 1, 2, 3$) denote the nearest-neighbors of the site i. However, when E_i in (3.1.9) includes a number of Ising spins, it is not so easy to write the corresponding exact relation. Furthermore, for higher spin ($S > 1/2$) systems as well as random spin-1/2 systems, it is a difficult task to find such exact relations.

As is understood from (3.1.16) or (3.1.15), the use of the kinematic relations for the spin operators is a crucial step in the theory based on the identity (3.1.9) or (3.1.12) as an average over a finite polynomial spin operators belonging to the neighboring sites. This can be systematically and easily achieved by the use of a differential operator technique introduced by Honmura and Kaneyoshi (Honmura & Kaneyoshi, 1979):

$$\tanh(\beta E_i) = \exp(E_i \nabla) \tanh x|_{x=0} \tag{3.1.17}$$

for (3.1.9) or

$$B_s(\beta E_i) = \exp(E_i \nabla) B_s(x)|_{x=0} \tag{3.1.18}$$

for (3.1.12), where $\nabla = \partial/\partial x$ is a differential operator. Here, we used the mathematical relation

$$\exp(a\nabla)\varphi(x) = \varphi(x + a) \tag{3.1.19}$$

This can be seen by expanding the exponential term in Taylor series

$$e^{a\nabla}\varphi(x) = [1 + a\nabla + \frac{a^2}{2!}\nabla^2 + ...]\varphi(x) = \varphi(x) + a\nabla\varphi(x) + \frac{a^2}{2!}\nabla^2\varphi(x) + ...$$

In the following parts, let us examine at first the simplest case of $\mu_i = \pm 1$ ($S =$

1/2). We will also examine the case of an arbitrary spin ($S > 1/2$) in the following sections.

Noticing that

$$e^{a\mu_i} = \cosh a + \mu_i \sinh a \tag{3.1.20}$$

Equation (3.1.17) can be written as, for $h = 0$

$$\tanh\left(\beta J \sum_{\delta} \mu_{i+\delta}\right) = \prod_{\delta=1}^{q} [\cosh(J\nabla) + \mu_{i+\delta} \sinh(J\nabla)] \tanh x|_{x=0} \tag{3.1.21}$$

Here, when $q = 1, 2$, or 3, the same exact relations as those of (3.1.15) can be easily derived. For example, when $q = 2$

$$\begin{aligned}
\tanh[K(\mu_{i+1} + \mu_{i+2})] &= [\cosh(J\nabla) + \mu_{i+1} \sinh(J\nabla)] \\
&\quad \times [\cosh(J\nabla) + \mu_{i+2} \sinh(J\nabla)] \tanh x|_{x=0} \\
&= (\mu_{i+1} + \mu_{i+2}) \sinh(J\nabla) \cosh(J\nabla) \tanh x|_{x=0} \\
&= \frac{1}{4}(\mu_{i+1} + \mu_{i+2})(e^{2J\nabla} - e^{-2J\nabla}) \tanh x|_{x=0} \\
&= B(\mu_{i+1} + \mu_{i+2})
\end{aligned} \tag{3.1.22}$$

Here, going from the second line to the third line in (3.1.22), we used the fact that even functions of ∇ must be zero when operating to the odd function (or $\tanh x$). In this way, the exact relation (3.1.10) can be generally rewritten as

$$\begin{aligned}
\langle \{f_i\} \mu_i \rangle &= \langle \{f_i\} e^{E_i \nabla} \rangle \tanh(\beta x)|_{x=0} \\
&= \langle \{f_i\} \prod_j [\cosh(J_{ij}\nabla) + \mu_j \sinh(J_{ij}\nabla)] \rangle \tanh[\beta(x+h)]|_{x=0}
\end{aligned} \tag{3.1.23}$$

This is also exact and is valid for any lattice structure of a spin-1/2 Ising model. Equation (3.1.23) can generate many kinds of identities for spin correlation functions, upon substituting appropriate Ising variable functions for $\{f_i\}$.

For the latter discussion, let us via equation (3.1.23) examine the spin

correlation function of the spin-1/2 linear chain with nearest-neighbor interaction J. Putting $\{f_i\} = \mu_k (k \neq i)$ and $h = 0$ into (3.1.23), it gives

$$\langle \mu_k \mu_i \rangle = \frac{1}{2} \tanh(2\beta J)(\langle \mu_k \mu_{i-1} \rangle + \langle \mu_k \mu_{i+1} \rangle) \tag{3.1.24}$$

At this place, due to translational invariance, the correlation function $\langle \mu_k \mu_i \rangle$ depends only on the distance between i and k:

$$\langle \mu_k \mu_i \rangle = \langle \mu_0 \mu_{i-k} \rangle = \langle \mu_0 \mu_r \rangle = g(r) \tag{3.1.25}$$

where $r = i - k$ is a measure of the distance between spins, in units of a lattice constant. Using (3.1.25), equation (3.1.24) can be written as

$$2 \coth(2\beta J) = \frac{g(r+1)}{g(r)} + \left[\frac{g(r)}{g(r-1)} \right]^{-1} \tag{3.1.26}$$

which implies that the right-hand side must be independent of r. Assuming that

$$\frac{g(r+1)}{g(r)} = \frac{g(r)}{g(r-1)} = \gamma \tag{3.1.27}$$

and taking the physically acceptable solution, the solution of (3.1.26) is given by

$$\gamma = \tanh(\beta J) \tag{3.1.28}$$

Thus, one obtains

$$g(r) = g_{i-k} = [\tanh(\beta J)]^r \tag{3.1.29}$$

This is a well-known exact result for the Ising chain.

3.2 Effective-Field Theories

It is well known in statistical mechanics that the one dimensional nearest-neighbor Ising model can be solved exactly. The exact solutions of the thermodynamic properties in the spin-1/2 Ising linear chain can be also derived

by the use of the differential operator technique based on the exact identities. As guides to real (two-or three-dimensional) systems, however, such a model has a serious disadvantage, since it does not have a phase transition at a non-zero temperature.

On the other hand, the first step in the interpretation of the magnetic properties of a solid is usually the application of an effective-field theory. When used correctly, the theory can be relied on for an approximate description of the major aspects of the phenomena being studied. It acts as a guidepost, as it was, indicating the direction of more elaborate theoretical contractions and of more detailed experiments. In this section, we discuss how the approximate formulations (or effective-field theories) superior to the mean-field approximation can be derived systematically from the present formulation based on the Ising spin identities.

3.2.1 Decoupling (or Zernike) approximation

As is understood from (3.1.16), the right-hand side of (3.1.23) contains thermal averages of multiple correlation functions. To proceed further, one has to make some approximations, in order to treat the identities approximately. The simplest approximation, and the most frequently adopted, is to decouple these according to

$$\langle \mu_j \mu_k ... \mu_l \rangle \approx \langle \mu_j \rangle \langle \mu_k \rangle ... \langle \mu_l \rangle \tag{3.2.1}$$

for $j \neq k \neq ... \neq l$

Introducing the approximation (3.2.1), the averaged value of μ_i (3.1.23 with $\{f_i\} = 1$) can be written in a compact form

$$\langle \mu_i \rangle = \prod_j [\cosh(J_{ij}\nabla) + \langle \mu_j \rangle \sinh(J_{ij}\nabla)] \tanh[\beta(x+h)]|_{x=0} \tag{3.2.2}$$

To simplify the notation, let us consider the case of zero-field and nearest-neighbor

interactions. For a ferromagnet with a coordination number q, equation (3.2.2) then reduces to

$$m = \langle \mu_i \rangle = [\cosh(J\nabla) + m \sinh(J\nabla)]^q \tanh(\beta x)|_{x=0} \tag{3.2.3}$$

The transition temperature T_c can be obtained by linearizing (3.2.3); by expanding the right-hand side of (3.2.3) and taking only the linear term of m, one obtains

$$q \sinh(J\nabla) \cosh^{q-1}(J\nabla) \tanh(\beta_c x)|_{x=0} = 1 \tag{3.2.4}$$

where $\beta_c = 1/k_B T_c$. In particular, when $q = 6$ (or a simple cubic lattice), equation (3.2.4) reduces to

$$\tanh(6J\beta_c) + 4 \tanh(4J\beta_c) + 5 \tanh(2J\beta_c) = \frac{16}{3} \tag{3.2.5}$$

which is noting but the result obtained by Zernike by means of another approach (Zernike, 1940). The transition temperature T_c is then given by

$$\frac{k_B T_c}{J} = 5.073 \qquad \text{for} \qquad q = 6 \tag{3.2.6}$$

which is superior to the MFA result

$$\frac{k_B T_c}{J} = q \tag{3.2.7}$$

We are now in a position to clarify the background why the simple decoupling approximation (Kaneyoshi et al, 1992b) improves the standard MFA (Berlin & Kac, 1952). For $h = 0$, equation (3.2.2) can be also rewritten as follows:

$$\langle \mu_i \rangle = \prod_j \left[\frac{1}{2}(1 + \langle \mu_j \rangle) e^{J_{ij}\nabla} + \frac{1}{2}(1 - \langle \mu_j \rangle) e^{-J_{ij}\nabla} \right] \tanh(\beta x)|_{x=0} \tag{3.2.8}$$

Here, the factors $(1/2)(1 + \langle \mu_j \rangle)$ and $(1/2)(1 - \langle \mu_j \rangle)$ mean the probabilities of a neighboring spin μ_j being up or down. Then, exponential operators $\exp(J_{ij}\nabla)$ and $\exp(-J_{ij}\nabla)$ express in a sense $\exp(J_{ij}\nabla)$ for $\mu_i = +1$ and $\exp(-J_{ij}\nabla)$ for $\mu_i = -1$, respectively. On the other hand, the standard MFA consist of assuming

that the field at the site i is $\langle E_i \rangle = \sum_j J_{ij} \langle \mu_j \rangle$ independent of the orientation of μ_i. This is clearly an approximation, for if μ_i is up, its neighbors μ_j will have more than average production for being up, a fluctuation effect that is neglected in the MFA. Thus, the partial correlation is included automatically in the simple framework through the usage of (3.1.20).

When one takes long-range interactions and the number of nearest-neighbors goes to infinite, it is known that the MFA becomes to be exact. Within the present framework, let us here show this fact. For this aim, we take the exchange interaction J_{ij} in (3.2.2) as

$$J_{ij} = \frac{j}{N} \qquad (j = \text{a finite constant}) \tag{3.2.9}$$

where N is the total number of lattice points. Then, equation (3.2.2) reduces to

$$m = \langle \mu_i \rangle = \left[\cosh\left(\frac{j}{N}\nabla\right) + m \sinh\left(\frac{j}{N}\nabla\right) \right]^{N-1} \tanh[\beta(x+h)]|_{x=0} \tag{3.2.10}$$

For a large values of N, $\cosh(j\nabla/N)$ and $\sinh(j\nabla/N)$ can be approximated as

$$\cosh\left(\frac{j}{N}\nabla\right) \approx 1 \qquad \text{and} \qquad \sinh\left(\frac{j}{N}\nabla\right) \approx \frac{j}{N}\nabla$$

so that equation (3.2.10) reduces to

$$m = \left[1 + m\frac{j}{N}\nabla \right]^{N-1} \tanh[\beta(x+h)]|_{x=0} \tag{3.2.11}$$

For $N \to \infty$, equation (3.2.11) is given by

$$m = e^{N[m(j/N)\nabla]} \tanh[\beta(x+h)]|_{x=0} = \tanh[\beta(mj+h)] \tag{3.2.12}$$

Thus, the MFA result can be derived from the present framework, when $N \to \infty$.

Finally, it will be fair to note some historical developments related to the framework of this part in the spin-1/2 Ising model. In order to treat the multi-spin correlation functions which appear for reducing the transcendental function

to a polynomial form (or 3.1.15), the decoupling approximation (3.2.1) was also introduced by Matsudaira (Matsudaira, 1973). He called it the first-order approximation. As noted above, the same decoupling approximation has been introduced into the present framework. It has been called the effective-field theory with correlations (EFT). The differential operator technique can be also rewritten in terms of the functional integration method (Kaneyoshi, 1980). Within the same framework as that of the EFT (or (3.2.1)), the method has been used by Lodz group (Mielnicki et al, 1986). Later, the same method as that of Matsudaira was proposed by Boccara (Boccara, 1983), who was apparently unaware of these earlier works, and it has subsequently been used extensively by him and group of researchers in Morocco as the finite cluster approximation (Boccara & Benyoussef, 1983). Clearly, as far as the physics concerned, it is immaterial whether one uses Matsudaira's first-order approximation, the EFT, the functional integration methods or the finite cluster approximation. All of them correspond to the Zernike approximation. However, in these methods, the differential operator technique has generally been more favored, because of the relative easiness of the formulation of other thermodynamic properties and the extension to higher spin problems as well as disordered spin systems.

3.2.2 Correlated effective-field (or Bethe-Peierls) approximation

In previous section, we have introduced a simple decoupling method (3.2.1) for treating the multi-spin correlation functions. In this part, we shall discuss how the formulation of previous section can be improved to a better one (or from Zernike to Bethe-Peierls approximation).

Let us now assume that the nearest-neighbor Ising variable $\mu_{i+\delta}$ can be related to the central spin μ_i via

$$\mu_{i+\delta} = \langle \mu_{i+\delta} \rangle + \lambda(\mu_i - \langle \mu_i \rangle) \tag{3.2.13}$$

where λ is a temperature dependent parameter. It is basically a measure of the

short-range order, or pair correlation parameter.

When equation (3.2.13) is substituted into the Hamiltonian (3.1.1) with $h = 0$, it is given by, for a system with nearest-neighbor interaction J

$$H = -\sum_i H_i^{eff}\mu_i + \text{constant term} \tag{3.2.14}$$

with

$$H_i^{eff} = J\sum_j \langle\mu_j\rangle - \lambda Jq\langle\mu_i\rangle = H_i^{mol} - R\langle\mu_i\rangle \tag{3.2.15}$$

where $R = \lambda Jq$ is the parameter which has to be determined at the end of calculation in some way. This transformation to the one-body Hamiltonian (3.2.15) has been introduced by Lines (Lines, 1974) and then the effective-field H_i^{eff} is modified by a term $R\langle\mu_i\rangle$ from the standard mean-field H_i^{mol}.

This revision of the effective field is closely related to the fundamental concept introduced by Onsager for dielectrics (Onsager, 1936). He has discussed that the orienting part of the local field on a given dipole (or the cavity field) should not include the contribution arising from the part of the polarization of dipoles in its vicinity which comes from its instantaneous orientation (or the reaction field). Namely, the cavity field is then obtained from the total mean field by subtracting the mean reaction field

$$E_i^{cavity} = \langle E_i\rangle - R\langle\mu_i\rangle \tag{3.2.16}$$

Thus, the effective field (3.2.15) is nothing but the cavity field (3.2.16) and the term $R\langle\mu_i\rangle$ corresponds to the reaction field. In the Lines method, the parameter λ (or R) has been determined at the end of the calculation by imposing consistency of the theory with the sum rule for the susceptibility. However, the method gives an accuracy essentially equivalent to that of the spherical model (Berlin & Kac, 1952), and unfortunately the sum rule is valid often only in the parametric phase and in the absence of strong fields. Moreover, when the method is applied to the two-dimensional ferromagnetic Ising lattice, it generally predicts $T_c = 0$.

In the differential operator technique, on the other hand, the concept (3.2.15)

has been used for evaluating the multi-spin correlation functions (Kaneyoshi et al, 1981; Kaneyoshi & Tamura, 1982; Honmura, 1984). This is sharply in contrast to the above approach. Then, the parameter λ has been determined self-consistently using the correlation function (3.1.23).

Substituting (3.2.13) into (3.1.23) with $\{f_i\} = 1$ and taking the nearest-neighbor interactions, one obtains, on assuming that $m = \langle\mu_i\rangle = \langle\mu_{i+\delta}\rangle$ and $h = 0$

$$
\begin{aligned}
m &= \langle\{P(m; J\nabla) + \lambda[\cosh(J\nabla) + \mu_i \sinh(J\nabla)]\}^q\rangle \tanh(\beta x)|_{x=0} \\
&= \langle[P(m; J\nabla) + \lambda e^{\mu_i J\nabla}]^q\rangle \tanh(\beta x)|_{x=0} \\
&= \sum_{\nu=0}^{q} \frac{q!}{\nu!(q-\nu)!} \lambda^\nu [P(m; J\nabla)]^{q-\nu} \langle e^{\mu_i \nu J\nabla}\rangle \tanh(\beta x)|_{x=0} \qquad (3.2.17) \\
&= \sum_{\nu=0}^{q} \frac{q!}{\nu!(q-\nu)!} \lambda^\nu [P(m; J\nabla)]^{q-\nu} [\cosh(\nu J\nabla) + m \sinh(\nu J\nabla)] \tanh(\beta x)|_{x=0}
\end{aligned}
$$

with

$$
P(m; J\nabla) = (1-\lambda)[\cosh(J\nabla) + m \sinh(J\nabla)] \qquad (3.2.18)
$$

Here, when $\lambda = 0$, equation (3.2.17) reduces to (3.2.3).

For the evaluation of λ, on the other hand, let us use the two spin correlation function which is given by, on putting $\{f_i\} = \mu_{i+\delta}$ into (3.1.23).

$$
\begin{aligned}
\langle\mu_{i+\delta}\mu_i\rangle &= \langle[\sinh(J\nabla) + \mu_{i+\delta} \cosh(J\nabla)] \\
&\quad \times \prod_{\delta'(\neq\delta)} [\cosh(J\nabla) + \mu_{i+\delta'} \sinh(J\nabla)]\rangle \tanh(\beta x)|_{x=0} \qquad (3.2.19)
\end{aligned}
$$

Substituting (3.2.13) into (3.2.19), one obtains

$$
\begin{aligned}
\langle\mu_{i+\delta}\mu_i\rangle &= m^2 + \lambda(1-m^2) = \langle[P(m; J\nabla) + \lambda\mu_i e^{\mu_i J\nabla}] \\
&\quad \times [P(m; J\nabla) + \lambda e^{\mu_i J\nabla}]^{q-1}\rangle \tanh(\beta x)|_{x=0}
\end{aligned}
$$

$$= \sum_{\nu=0}^{q-1} \frac{(q-1)!}{\nu!(q-1-\nu)!} \lambda^{\nu} P(m; J\nabla)[P(m; J\nabla)]^{q-1-\nu} \tag{3.2.20}$$

$$\times [\cosh(\nu J\nabla) + m \sinh(\nu J\nabla)] \tanh(\beta x)|_{x=0} + \sum_{\nu=0}^{q-1} \frac{(q-1)!}{\nu!(q-1-\nu)!} \lambda^{\nu+1}$$

$$\times [P(m; J\nabla)]^{q-1-\nu} [m \cosh((\nu+1)J\nabla) + \sinh((\nu+1)J\nabla)] \tanh(\beta x)|_{x=0}$$

with

$$P(m; J\nabla) = (1-\lambda)[m \cosh(J\nabla) + \sinh(J\nabla)] \tag{3.2.21}$$

Thus, the magnetization m and correlated parameter λ of the Ising ferromagnet with a coordination number q can be evaluated from the coupled equations (3.2.17) and (3.2.20).

For example, when $q = 4$ (or square lattice), they reduce to

$$m = 4(K_1 + 3K_2\lambda^2 - 2K_2\lambda^3)m + 4K_2(1 - 3\lambda^2 + 2\lambda^3)m^3 \tag{3.2.22}$$

and

$$\begin{aligned} m^2 + \lambda(1-m^2) = {} & K_1(1+3\lambda^2) + K_2\lambda^2(3+\lambda^2) \\ & + m^2[3K_1(1-\lambda^2) + K_2(3+3\lambda^2-8\lambda^3+2\lambda^4)] \\ & + m^4[1-6\lambda^2+8\lambda^3-3\lambda^4] \end{aligned} \tag{3.2.23}$$

where the coefficients K_1 and K_2 are given by

$$K_1 + \frac{1}{8}[\tanh(4\beta J) + 2\tanh(2\beta J)]$$

$$K_2 + \frac{1}{8}[\tanh(4\beta J) - 2\tanh(2\beta J)] \tag{3.2.24}$$

Thus, the transition temperature T_c can be determined from the coupled equations

$$1 = 4(K_1 + 3K_2\lambda^2 - 2K_2\lambda^3)$$

$$\lambda = K_1 + 3\lambda^2(K_1 + K_2) + K_2\lambda^4 \tag{3.2.25}$$

which can be solved analytically and gives

$$\frac{k_B T}{J} = \frac{2}{\ln 2} \qquad \text{and} \qquad \lambda(T = T_c) = \frac{1}{3} \tag{3.2.26}$$

The temperature dependence of λ for the ferromagnetic square lattice with nearest-neighbor interaction J is depicted in Fig. 3.1 by solving the coupled equations (3.2.21) and (3.2.22) numerically. In general, the transition temperature T_c and

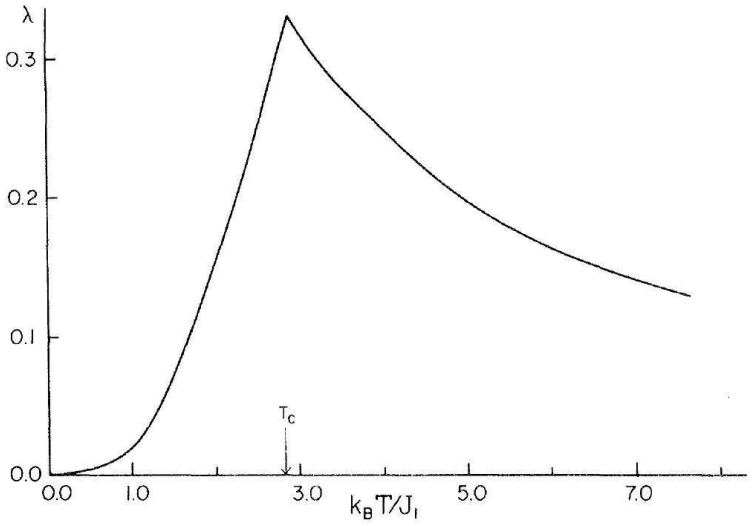

Figure 3.1 Temperature dependence of λ for the ferromagnetic square lattice, (Kaneyoshi, 1992).

the correlated parameter λ at $T = T_c$ are given by, within the present formulation (or 3.2.17 and (3.2.18)),

$$\frac{k_B T_c}{J} = \frac{2}{\ln[q/(q-2)]} \tag{3.2.27}$$

and

$$\lambda(T = T_c) = \frac{1}{q-1} \tag{3.2.28}$$

The result of T_c is equivalent to that of Bethe-Peierls approximation, although the philosophy on which these two theories are based is different to each other. For comparison, the values of T_c obtained from sections (3.2.1) and (3.2.2) as well as the MFA are collected in Table 3.1 and the exact or high-temperature series expansion results (Onsager, 1944) are also listed.

Table 3.1 Values of k_BT_c/J.

z	MFA	EFT (Zernike)	Bethe-Peierls	Exact
2	2.0	0.0	0.0	0.0
3	3.0	2.104	1.821	1.519
4	4.0	3.090	2.885	2.269
6	6.0	5.073	4.933	4.511
8	8.0	7.061	6.952	6.353
12	12.0	11.045	10.970	9.795

3.2.3 Effective-field renormalization group method

In previous sections we have discussed how the spin correlations can be decoupled for transforming the transcendental function into a polynomial form. Then, the results applicable to general lattice coordination numbers are obtained. However, the fault of these approaches is that the results depend on the coordination number, but not on the dimensionality. A value of $q = 4$, for example, may equally be a square lattice or a diamond lattice. In order to take into account of the lattice dimensionality as well as the coordination number, one has to treat the multi-spin correlation functions in forms depending on these qualities. Such a formulation can be made by going to Matsudaira's higher order decoupling approximation (Matsudaira, 1973) better than the simple decoupling approximation (Kaneyoshi et al, 1992b). Then, the formulation cannot be described in a general form but it must be made separately in a way of depending on the lattice structure. Another way of incorporating these properties is to express the thermal average of the transcendental function as an average over a finite polynomial of a spin operator in an $n - site$ cluster ($n > 1$) (Honmura & Kaneyoshi, 1979).

In this part, let us discuss how traditional (effective-field) procedures of obtaining equations of state can be converted into a modern tool for constructing a regular renormalization-group mapping according to Wilson ideas. Due to its

connection with standard mean-field procedure, the denomination of mean-field renormalization group has been used in the literature. It has been successfully used to provide qualitative and quantitative insights into the critical behavior of spin systems. On the other hand, the effective-field renormalization-group scheme can be, via the differential operator technique, formulated by treating the effects of the surrounding spins of each of the clusters in a way of constructing the effective-field equations of states on the basis of the Ising spin identities.

The principal of the phenomenological renormalization group is based on the comparison of two clusters of different sizes N, $N^{'}$ $(N^{'} < N)$, each of them simulating the infinite system. For the two clusters, one calculates an approximate equation of state for the magnetization per site, namely m_N and $m_{N'}$. In the mean-field renormalization group, this is done within the traditional mean-field scheme, in which the effects of the surrounding spins in each cluster is replaced by very small symmetric breaking fields b and $b^{'}$, acting on the boundary sites of each of the clusters with N and $N^{'}$ interacting spins, respectively. By imposing that both magnetizations of the clusters and respective symmetric braking fields are scaled in the same way, one gets

$$\frac{\partial m_N(K,b)}{\partial b}|_{b=0} = \frac{\partial m_{N'}(K^{'},b^{'})}{\partial b'}|_{b'=0} \tag{3.2.29}$$

which is independent of the scaling factor. This relation gives a recursion relation between the coupling constants K and $K^{'}$ in the systems. From the relation $K^{'} = K^{'}(K)$, the critical coupling K_c can be extracted by solving the fixed point equation $K^* = K^{'}(K^*)$ invariant under a change of scale. Furthermore, the critical exponent ν of the correlation length ξ defined by

$$\xi \propto |T - T_c|^{-\nu} \tag{3.2.30}$$

can also be obtained by linearizing the recursion relation in the neighborhood of the fixed point K^*:

$$\left(\frac{\partial K^{'}}{\partial K}\right)_{K=K'} = l^{1/\nu} \tag{3.2.31}$$

where $l = (N/N^{'})^{1/d}$ is the scaling factor and d is the dimensionality of the system.

Let us illustrate now the general arguments of the phenomenological renormalization group by taking the simplest choice, namely, clusters of one ($N^{'} = 1$) and two ($N = 2$) spins. In the one-spin cluster the spin μ_1 interacts with q_1 nearest-neighbor sites via the coupling constants $K_{ij}^{'}$. In the two spin cluster, on the other hand, the spins μ_1 and μ_2 interact directly via the coupling K_{12} and both μ_1 and μ_2 spins interact with their neighbor sites also via the coupling constants K_{1i} and $K_{2j}^{'}$. Using the same procedures as those of previous sections, the averaged magnetizations $m_{N'}$ and m_N associated to the $N^{'} = 1$ and $N = 2$ clusters are given by

$$m_{N'} = \langle \mu_1 \rangle = \left\langle \tanh \left(\sum_j K_{1j}^{'} \mu_j^{'} \right) \right\rangle \tag{3.2.32}$$

and

$$m_N = \left\langle \frac{1}{2}(\mu_1 + \mu_2) \right\rangle = \left\langle \frac{\sinh(u+v)}{\cosh(u+v) + \exp(-2K_{12})\cosh(u-v)} \right\rangle \tag{3.2.33}$$

where $u = \sum_j K_{1j}\mu_j$ and $v = \sum_{j'} K_{2j'}\mu_{j'}$.

Using the differential operator technique and noticing that the sites 1 and 2 of the two-spin cluster may include a set of common-neighbor sites, the set of equations (3.2.32) and (3.2.33) can be written in the following forms:

$$m_{N'} = \left\langle \prod_j \exp(K_{1j}^{'} \mu_j^{'} \nabla_x) \right\rangle f(x)|_{x=0} \tag{3.2.34}$$

and

$$m_N = \left\langle \prod_j^{'} \exp(K_{1j}\mu_j \nabla) \prod_{j'}^{'} \exp(K_{2j'}\mu_{j'}\nabla_y) \prod_k^{'} \exp[\mu_k(K_{1k}\nabla_x + K_{2k}\nabla_y)] \right\rangle$$

$$\times f(x,y)|_{x=0,y=0} \tag{3.2.35}$$

where $\nabla_\mu = \partial/\partial\mu$ ($\mu = x$ or y) are the differential operators and the

functions $f(x)$ and $f(x,y)$ are defined by

$$f(x) = \tanh x \tag{3.2.36}$$

and

$$f(x,y) = \frac{\sinh(x+y)}{\cosh(x+y) + \exp(-2K_{12})\cosh(x-y)} \tag{3.2.37}$$

Here, the products $\prod'$ over j and $j^{'}$ in equation (3.2.35) are respectively the isolated nearest-neighbor spins of sites 1 and 2, while the product $\prod'$ over k is restricted to the sites which are simultaneously nearest neighbors of both μ_1 and μ_2 spins. Furthermore, the exponential operators in (3.2.34) and (3.2.35) can be rewritten into the product forms of μ_j by the use of equation (3.1.20).

As discussed in Sec.(3.2.1), we introduce here the decoupling approximation (3.2.1) into the exact relations (3.2.34) and (3.2.35). Basing on the approximation (3.2.1) and replacing each boundary average $\langle \mu_{j'} \rangle$ (or $\langle \mu_j \rangle$) in their right-hand sides with the symmetry braking mean-field parameters $b_j^{'}$ (or b_j), the critical behavior of the system can be obtained by expanding the right-hand side of them and takin only first-order terms in these parameters

$$m_{N'}(K^{'}, b^{'}) = A_{N'}^{(q)}(K^{'})b^{'} + O(b^{'3}) \tag{3.2.38}$$

and

$$m_N(K,b) = A_N^{(q)}(K)b + O(b^3) \tag{3.2.39}$$

where the coefficients $A_{N'}^{(q)}(K^{'})$ and $A_N^{(q)}(K)$ for the $N^{'} = 1$ and $N = 2$ clusters are given, on assuming only the nearest-neighbor interactions ($K^{'}$ and K), by

$$A_{N'}^{(q)}(K^{'}) = q_1 \cosh^{q-1}(K\nabla_x) f(x)|_{x=0} \tag{3.2.40}$$

and

$$A_N^{(q)}(K) = \{2q^{'} \sinh(K\nabla_x)\cosh^{q^{'}-1}(K\nabla_x)\cosh^{q^{'}}(K\nabla_y)\cosh^{q^{''}}[K(\nabla_x+\nabla_y)]$$

$$+q^{''}\sinh[K(\nabla_x+\nabla_y)]\cosh^{q^{'}}(K\nabla_x)\cosh^{q^{'}}(K\nabla_y)$$

$$\times \cosh^{q''-1}[K(\nabla_x + \nabla_y)]\}f(x,y)|_{x=0,y=0} \tag{3.2.41}$$

Here, q' denotes the number of sites which are nearest-neighbors of μ_1 (or μ_2) but not neighboring to μ_2 (or μ_1), and q'' represents the number of sites that are simultaneously nearest neighbors of both μ_1 and μ_2. Thus, $q_2 = 2q' + q''$ is the total number of nearest-neighbor sites of the two-spin cluster. Hence, the coefficient $A_N^{(q)}(K)$ incorporates the detail of the geometry of the lattice beyond its coordination number q_1, through q' and q''.

Combining (3.2.40) and (3.2.41) with the scaling assumption, one gets from (3.2.29)

$$A_{N'}^{(q)}(K') = A_N^{(q)}(K) \tag{3.2.42}$$

which is the recursion relation between the coupling constants K and K' for the two rescaled systems $N' = 1$ and $N = 2$. The reduced critical interaction K_c is the non-trivial fixed point $K' = K = K^\star = K_c$ solution of (3.2.42) and the critical exponent ν for the correlation length can be obtained from (3.2.31), noting that

$$\left(\frac{\partial K'}{\partial K}\right)_{K=K} = \frac{\left(\frac{\partial A_N^{(q)}(K)}{\partial K}\right)_{K=K}}{\left(\frac{\partial A_{N'}^{(q)}(K')}{\partial K'}\right)_{K=K}} \tag{3.2.43}$$

These approaches can be also extended to higher-order approximate recursion relations by considering clusters larger than $N = 2$.

CHAPTER FOUR
THE INTRODUCED EFFECTIVE FIELD APPROXIMATION

4.1 Solutions for the Spin-1 BC Model in a Longitudinal Magnetic Field with Crystal Field

At first, we discuss how the theory can be formulated within the framework of the effective field theory with correlations. To do this, we consider a two dimensional lattice which has N identical spins arranged. On the lattice, we select a system which consists a central spin, labeled 0, and q perimeter spins being the nearest-neighbors of the central spin. The system consists of $(q+1)$ spins being independent from the value of S. The nearest-neighbor spins are in an effective field produced by the outer spins, which can be determined by the condition that the thermal average of the central spin is equal to that of its nearest-neighbor spins. The Hamiltonian of the spin-1 system in a longitudinal magnetic field is given by

$$H = -J \sum_{<i,j>} S_i^z S_j^z - D \sum_i (S_i^z)^2 - h \sum_i S_i^z \tag{4.1.1}$$

where, the first summation is over the nearest-neighbor pair of spins and the operator S_i^z takes the values of $S_i^z = \pm 1, 0$. J, D and h represent the exchange interaction, the single ion anisotropy (i.e. crystal field) and longitudinal magnetic field, respectively. By the use of the exact Van der Waerden identity (Balcerzak, 2002; Callen, 1963; Suzuki, 1965) for the spin-1 Ising ferromagnetic system with the coordination number q, the thermal average of the spin variables at the site i is given by

$$\langle \{f_i\} S_i^z \rangle = \left\langle \{f_i\} \exp\left(J \sum_{\delta}^{q} S_\delta^z \right) \nabla \right\rangle F(x) \mid_{x=0} \tag{4.1.2}$$

where, $\beta = 1/k_B T$ with absolute temperature T and Boltzmann constant k_B. $\nabla = \partial/\partial x$ is a differential operator, δ expresses the nearest-neighbor sites of the central spin and $\{f_i\}$ can be any function of the Ising variables as long as it is not

a function of the site. From equation (4.1.2) with $\{f_i\} = 1$, the thermal average of a central spin can be represented in the form for square ($q = 4$) lattice

$$m_0 = \langle S_0^z \rangle = \left\langle \prod_{\delta=1}^{4} [1 + S_\delta^z \sinh(J\nabla) + (S_\delta^z)^2 \{\cosh(J\nabla) - 1\}] \right\rangle F(x) \mid_{x=0} \quad (4.1.3)$$

$$\begin{aligned}
&= l_0 + 4k_1\langle S_1\rangle + 4(l_2 - l_0)\langle S_1^2\rangle + 6l_1\langle S_1S_2\rangle + 12(k_2 - k_1)\langle S_1S_2^2\rangle \\
&+6(l_0 - 2l_2 + l_3)\langle S_1^2S_2^2\rangle + 4k_3\langle S_1S_2S_3\rangle + 12(l_4 - l_1)\langle S_1S_2S_3^2\rangle \\
&+12(k_4 - 2k_2 + k_1)\langle S_1S_2^2S_3^2\rangle + 4(l_5 - 3l_3 + 3l_2 - l_0)\langle S_1^2S_2^2S_3^2\rangle \\
&+l_8\langle S_1S_2S_3S_4\rangle + 4(k_5 - k_3)\langle S_1S_2S_3S_4^2\rangle + 6(l_1 - 2l_4 + l_6)\langle S_1S_2S_3^2S_4^2\rangle \\
&+4(k_6 - 3k_4 + 3k_2 - k_1)\langle S_1S_2^2S_3^2S_4^2\rangle \\
&+(l_0 - 4l_2 + 6l_3 - 4l_5 + l_7)\langle S_1^2S_2^2S_3^2S_4^2\rangle
\end{aligned} \quad (4.1.4)$$

with the coefficients

$$k_1 = \sinh(J\nabla)F(x) \mid_{x=0}$$

$$k_2 = \sinh(J\nabla)\cosh(J\nabla)F(x) \mid_{x=0}$$

$$k_3 = \sinh^3(J\nabla)F(x) \mid_{x=0}$$

$$k_4 = \cosh^2(J\nabla)\sinh(J\nabla)F(x) \mid_{x=0}$$

$$k_5 = \sinh^3(J\nabla)\cosh(J\nabla)F(x) \mid_{x=0}$$

$$k_6 = \cosh^3(J\nabla)\sinh(J\nabla)F(x) \mid_{x=0}$$

$$l_0 = F(0)$$

$$l_1 = \sinh^2(J\nabla)F(x) \mid_{x=0}$$

$$l_2 = \cosh(J\nabla)F(x) \mid_{x=0}$$

$$l_3 = \cosh^2(J\nabla)F(x) \mid_{x=0}$$

$$l_4 = \sinh^2(J\nabla)\cosh(J\nabla)F(x)\mid_{x=0}$$

$$l_5 = \cosh^3(J\nabla)F(x)\mid_{x=0}$$

$$l_6 = \sinh^2(J\nabla)\cosh^2(J\nabla)F(x)\mid_{x=0}$$

$$l_7 = \cosh^4(J\nabla)F(x)\mid_{x=0}$$

$$l_8 = \sinh^4(J\nabla)F(x)\mid_{x=0}$$

These coefficients can be derived from a mathematical identity $\exp(\alpha\nabla)F(x) = F(x+\alpha)$. The function $F(x)$ for spin-1 Ising system is given by

$$F(x) = \frac{2\sinh[\beta(x+h)]}{2\cosh[\beta(x+h)] + \exp(-\beta D)} \tag{4.1.5}$$

Next, the average value of a perimeter-spin in the system can be written as follow and it is found as

$$\begin{aligned} m_1 &= \langle S_\delta^z \rangle \\ &= \langle \exp(JS_0^z + (q-1)A)\nabla \rangle F(x)\mid_{x=0} \\ &= \langle [1 + S_0^z \sinh(J\nabla) + (S_0^z)^2\{\cosh(J\nabla) - 1\}] \rangle F(x+\gamma)\mid_{x=0} \end{aligned} \tag{4.1.6}$$

$$m_1 = \langle S_1 \rangle = a_1(1 - \langle S_0^2 \rangle) + a_2\langle S_0 \rangle + a_3\langle S_0^2 \rangle \tag{4.1.7}$$

with

$$a_1 = F(\gamma)$$

$$a_2 = \sinh(J\nabla)F(x+\gamma)\mid_{x=0}$$

$$a_3 = \cosh(J\nabla)F(x+\gamma)\mid_{x=0}$$

where $\gamma = (q-1)A$ is the effective field produced by the $(q-1)$ spins outside the system and A is an unknown parameter to be determined self-consistently.

In the effective-field approximation, the number of independent spin variables describes the considered system. This number is given by the relation $\nu = \langle (S_i^z)^{2S} \rangle$. As an example, for spin-1 system $2S = 2$, which means that we have to introduce the additional parameters, $\langle (S_\delta^z)^2 \rangle$ and $\langle (S_0^z)^2 \rangle$ resulting from the usage of the Van der Waerden identity for the spin-1 Ising system.

$$\langle (S_0^z)^2 \rangle = \left\langle \prod_{\delta=1}^{4} [1 + S_\delta^z \sinh(J\nabla) + (S_\delta^z)^2 \{\cosh(J\nabla) - 1\}] \right\rangle G(x) \mid_{x=0} \tag{4.1.8}$$

$$\begin{aligned}
\langle S_0^2 \rangle = {} & p_0 + 4n_1 \langle S_1 \rangle + 4(p_2 - p_0) \langle S_1^2 \rangle + 6p_1 \langle S_1 S_2 \rangle + 12(n_2 - n_1) \langle S_1 S_2^2 \rangle \\
& + 6(p_0 - 2p_2 + p_3) \langle S_1^2 S_2^2 \rangle + 4n_3 \langle S_1 S_2 S_3 \rangle + 12(p_4 - p_1) \langle S_1 S_2 S_3^2 \rangle \\
& + 12(n_1 - 2n_2 + n_4) \langle S_1 S_2^2 S_3^2 \rangle + 4(p_5 - 3p_3 + 3p_2 - p_0) \langle S_1^2 S_2^2 S_3^2 \rangle \\
& + p_8 \langle S_1 S_2 S_3 S_4 \rangle + 4(n_5 - n_3) \langle S_1 S_2 S_3 S_4^2 \rangle \\
& + 6(p_1 - 2p_4 + p_6) \langle S_1 S_2 S_3^2 S_4^2 \rangle \\
& + 4(n_6 - 3n_4 + 3n_2 - n_1) \langle S_1 S_2^2 S_3^2 S_4^2 \rangle \\
& + (p_0 - 4p_2 + 6p_3 - 4p_5 + p_7) \langle S_1^2 S_2^2 S_3^2 S_4^2 \rangle
\end{aligned} \tag{4.1.9}$$

with the coefficients

$$n_1 = \sinh(J\nabla) G(x) \mid_{x=0}$$

$$n_2 = \sinh(J\nabla) \cosh(J\nabla) G(x) \mid_{x=0}$$

$$n_3 = \sinh^3(J\nabla) G(x) \mid_{x=0}$$

$$n_4 = \cosh^2(J\nabla) \sinh(J\nabla) G(x) \mid_{x=0}$$

$$n_5 = \sinh^3(J\nabla) \cosh(J\nabla) G(x) \mid_{x=0}$$

$$n_6 = \cosh^3(J\nabla) \sinh(J\nabla) G(x) \mid_{x=0}$$

$$p_0 = G(0)$$

$$p_1 = \sinh^2(J\nabla)G(x)\mid_{x=0}$$

$$p_2 = \cosh(J\nabla)G(x)\mid_{x=0}$$

$$p_3 = \cosh^2(J\nabla)G(x)\mid_{x=0}$$

$$p_4 = \sinh^2(J\nabla)\cosh(J\nabla)G(x)\mid_{x=0}$$

$$p_5 = \cosh^3(J\nabla)G(x)\mid_{x=0}$$

$$p_6 = \sinh^2(J\nabla)\cosh^2(J\nabla)G(x)\mid_{x=0}$$

$$p_7 = \cosh^4(J\nabla)G(x)\mid_{x=0}$$

$$p_8 = \sinh^4(J\nabla)G(x)\mid_{x=0}$$

where the function $G(x)$ is defined by

$$G(x) = \frac{2\cosh[\beta(x+h)]}{2\cosh[\beta(x+h)] + \exp(-\beta D)} \tag{4.1.10}$$

Corresponding to (4.1.6),

$$\langle (S_\delta^z)^2 \rangle = \langle [1 + S_0^z \sinh(J\nabla) + (S_0^z)^2\{\cosh(J\nabla) - 1\}]\rangle G(x+\gamma)\mid_{x=0} \tag{4.1.11}$$

$$\langle S_1^2 \rangle = b_1 + b_2\langle S_0\rangle + (b_3 - b_1)\langle S_0^2\rangle \tag{4.1.12}$$

with

$$b_1 = G(\gamma)$$

$$b_2 = \sinh(J\nabla)G(x+\gamma)\mid_{x=0}$$

$$b_3 = \cosh(J\nabla)G(x+\gamma)\mid_{x=0}$$

A detailed derivation of the functions $F(x)$ and $G(x)$ in (4.1.5) and (4.1.10) are given in Appendix.

When the right hand sides of the equations (4.1.3), (4.1.6), (4.1.8) and (4.1.11) are expanded, the multispin correlation functions may be obtained. The simplest approximation, and one of the most frequently adopted is to decouple these equations (Tamura & Kaneyoshi, 1981) according to

$$\left\langle S_i^z (S_j^z)^2 ... S_l^z \right\rangle \cong \langle S_i^z \rangle \left\langle (S_j^z)^2 \right\rangle ... \langle S_l^z \rangle \tag{4.1.13}$$

for $i \neq j \neq ... \neq l$. The main difference of the method used in this study, from other approximations in the literature can be emerged in comparison with any DA when expanding the right-hand sides of equations (4.1.3), (4.1.6), (4.1.8) and (4.1.11).

For the spin-1 Ising system with $q = 4$, taking as a basis the equations (4.1.4), (4.1.7), (4.1.9) and (4.1.12), we have derived the set of linear equations of the spin correlation functions which interact in the system. It has been considered that (i) the correlations are depended only on the distance between the spins, (ii) the average values of a central spin and its nearest-neighbor spin (it is labeled as the perimeter spin) are equal to each other, and (iii) in the matrix representations of spin operator $\hat{S}$, the spin-1 system has the properties $(S_\delta^z)^3 = S_\delta^z$ and $(S_\delta^z)^4 = (S_\delta^z)^2$. Thus, the number of the set of linear equations obtained for the spin-1 Ising system with $q = 4$ reduces to thirty four linear equations:

$$\begin{aligned}
\langle S_0^z \rangle = {} & l_0 + 4k_1\langle S_1 \rangle + 4(l_2 - l_0)\langle S_1^2 \rangle + 6l_1\langle S_1 S_2 \rangle \\
& + 12(k_2 - k_1)\langle S_1 S_2^2 \rangle + 6(l_0 - 2l_2 + l_3)\langle S_1^2 S_2^2 \rangle + 4k_3\langle S_1 S_2 S_3 \rangle \\
& + 12(l_4 - l_1)\langle S_1 S_2 S_3^2 \rangle + 12(k_1 - 2k_2 + k_4)\langle S_1 S_2^2 S_3^2 \rangle \\
& + 4(l_5 - 3l_3 + 3l_2 - l_0)\langle S_1^2 S_2^2 S_3^2 \rangle + l_8\langle S_1 S_2 S_3 S_4 \rangle \\
& + 4(k_5 - k_3)\langle S_1 S_2 S_3 S_4^2 \rangle + 6(l_1 - 2l_4 + l_6)\langle S_1 S_2 S_3^2 S_4^2 \rangle \\
& + 4(k_6 - 3k_4 + 3k_2 - k_1)\langle S_1 S_2^2 S_3^2 S_4^2 \rangle \\
& + (l_0 - 4l_2 + 6l_3 - 4l_5 + l_7)\langle S_1^2 S_2^2 S_3^2 S_4^2 \rangle
\end{aligned}$$

$$\begin{aligned}
\langle S_1 S_0\rangle &= (4l_2 - 3l_0)\langle S_1\rangle + 4k_1\langle S_1^2\rangle + 6(l_0 + l_1 - 2l_2 + l_3)\langle S_1 S_2^2\rangle \\
&\quad +12(k_2 - k_1)\langle S_1^2 S_2^2\rangle + 4k_3\langle S_1 S_2 S_3^2\rangle \\
&\quad +4(l_5 + 3l_4 - 3l_3 + 3l_2 - 3l_1 - l_0)\langle S_1 S_2^2 S_3^2\rangle \\
&\quad +12(k_1 - 2k_2 + k_4)\langle S_1^2 S_2^2 S_3^2\rangle + l_8\langle S_1 S_2 S_3 S_4^2\rangle \\
&\quad +4(k_5 - k_3)\langle S_1 S_2 S_3^2 S_4^2\rangle \\
&\quad +(l_0 + 6l_1 - 4l_2 + 6l_3 - 12l_4 - 4l_5 + 6l_6 + l_7)\langle S_1 S_2^2 S_3^2 S_4^2\rangle \\
&\quad +4(k_6 - 3k_4 + 3k_2 - k_1)\langle S_1^2 S_2^2 S_3^2 S_4^2\rangle \\
\langle S_1 S_2 S_0\rangle &= (3l_0 + 6l_1 - 8l_2 + 6l_3)\langle S_1 S_2\rangle + 4(3k_2 - 2k_1)\langle S_1 S_2^2\rangle \\
&\quad +4(3k_1 - 6k_2 + k_3 + 3k_4)\langle S_1 S_2^2 S_3^2\rangle \\
&\quad +4(l_5 + 3l_4 - 3l_3 + 3l_2 - 3l_1 - l_0)\langle S_1 S_2 S_3^2\rangle \\
&\quad +(l_0 + 6l_1 - 4l_2 + 6l_3 - 12l_4 - 4l_5 + 6l_6 + l_7 + l_8)\langle S_1 S_2 S_3^2 S_4^2\rangle \\
&\quad +4(k_6 + k_5 - 3k_4 - k_3 + 3k_2 - k_1)\langle S_1 S_2^2 S_3^2 S_4^2\rangle \\
\langle S_1 S_2 S_3 S_0\rangle &= (4l_5 + 12l_4 - 6l_3 + 4l_2 - 6l_1 - l_0)\langle S_1 S_2 S_3\rangle \\
&\quad +4(k_1 - 3k_2 + k_3 + 3k_4)\langle S_1 S_2 S_3^2\rangle \\
&\quad +(l_0 + 6l_1 - 4l_2 + 6l_3 - 12l_4 - 4l_5 + 6l_6 + l_7 + l_8)\langle S_1 S_2 S_3 S_4^2\rangle \\
&\quad +4(k_6 + k_5 - 3k_4 - k_3 + 3k_2 - k_1)\langle S_1 S_2 S_3^2 S_4^2\rangle \\
\langle S_1\rangle &= a_1 + a_2\langle S_0\rangle + (a_3 - a_1)\langle S_0^2\rangle \\
\langle S_1 S_2\rangle &= a_1\langle S_1\rangle + a_2\langle S_1 S_0\rangle + (a_3 - a_1)\langle S_1 S_0^2\rangle \\
\langle S_1 S_2 S_3\rangle &= a_1\langle S_1 S_2\rangle + a_2\langle S_1 S_2 S_0\rangle + (a_3 - a_1)\langle S_1 S_2 S_0^2\rangle \\
\langle S_1 S_2 S_3 S_4\rangle &= a_1\langle S_1 S_2 S_3\rangle + a_2\langle S_1 S_2 S_3 S_0\rangle + (a_3 - a_1)\langle S_1 S_2 S_3 S_0^2\rangle \\
\langle S_1^2\rangle &= b_1 + b_2\langle S_0\rangle + (b_3 - b_1)\langle S_0^2\rangle \\
\langle S_1 S_2^2\rangle &= b_1\langle S_1\rangle + b_2\langle S_1 S_0\rangle + (b_3 - b_1)\langle S_1 S_0^2\rangle \\
\langle S_1^2 S_2^2\rangle &= b_1\langle S_1^2\rangle + b_2\langle S_1^2 S_0\rangle + (b_3 - b_1)\langle S_1^2 S_0^2\rangle
\end{aligned}$$

$$\langle S_1S_2S_3^2\rangle = b_1\langle S_1S_2\rangle + b_2\langle S_1S_2S_0\rangle + (b_3-b_1)\langle S_1S_2S_0^2\rangle$$

$$\langle S_1S_2^2S_3^2\rangle = b_1\langle S_1S_2^2\rangle + b_2\langle S_1S_2^2S_0\rangle + (b_3-b_1)\langle S_1S_2^2S_0^2\rangle$$

$$\langle S_1^2S_2^2S_3^2\rangle = b_1\langle S_1^2S_2^2\rangle + b_2\langle S_1^2S_2^2S_0\rangle + (b_3-b_1)\langle S_1^2S_2^2S_0^2\rangle$$

$$\langle S_1S_2S_3S_4^2\rangle = a_1\langle S_1S_2S_3S_4\rangle + a_2\langle S_0S_1S_2S_3^2\rangle + (a_3-a_1)\langle S_1S_2S_3^2S_0^2\rangle$$

$$\langle S_1S_2S_3^2S_4^2\rangle = a_1\langle S_1S_2S_3S_4^2\rangle + a_2\langle S_0S_1S_2S_3\rangle + (a_3-a_1)\langle S_1S_2S_3S_0^2\rangle$$

$$\langle S_1S_2^2S_3^2S_4^2\rangle = a_1\langle S_1S_2S_3^2S_4^2\rangle + a_2\langle S_0S_1S_2S_3^2\rangle + (a_3-a_1)\langle S_1S_2S_3^2S_0^2\rangle$$

$$\langle S_1^2S_2^2S_3^2S_4^2\rangle = a_1\langle S_1S_2^2S_3^2S_4^2\rangle + a_2\langle S_0S_1S_2^2S_3^2\rangle + (a_3-a_1)\langle S_1S_2^2S_3^2S_0^2\rangle$$

$$\langle S_0S_1^2\rangle = b_3\langle S_0\rangle + b_2\langle S_0^2\rangle$$

$$\langle S_0S_1S_2^2\rangle = b_3\langle S_0S_1\rangle + b_2\langle S_1S_0^2\rangle\rangle$$

$$\langle S_0S_1^2S_2^2\rangle = b_3\langle S_0S_1^2\rangle + b_2\langle S_1^2S_0^2\rangle$$

$$\langle S_0S_1S_2S_3^2\rangle = b_3\langle S_0S_1S_2\rangle + b_2\langle S_1S_2S_0^2\rangle$$

$$\langle S_0S_1S_2^2S_3^2\rangle = b_3\langle S_0S_1S_2^2\rangle + b_2\langle S_1S_2^2S_0^2\rangle$$

$$\langle S_0S_1^2S_2^2S_3^2\rangle = b_3\langle S_0S_1^2S_2^2\rangle + b_2\langle S_1^2S_2^2S_0^2\rangle$$

$$\begin{aligned}\langle S_0^2\rangle = {} & p_0 + 4n_1\langle S_1\rangle + 4(p_2-p_0)\langle S_1^2\rangle + 6p_1\langle S_1S_2\rangle + 12(n_2-n_1)\langle S_1S_2^2\rangle \\ & +6(p_0-2p_2+p_3)\langle S_1^2S_2^2\rangle + 4n_3\langle S_1S_2S_3\rangle + 12(p_4-p_1)\langle S_1S_2S_3^2\rangle \\ & +12(n_1-2n_2+n_4)\langle S_1S_2^2S_3^2\rangle + 4(p_5-3p_3+3p_2-p_0)\langle S_1^2S_2^2S_3^2\rangle \\ & +p_8\langle S_1S_2S_3S_4\rangle + 4(n_5-n_3)\langle S_1S_2S_3S_4^2\rangle \\ & +6(p_1-2p_4+p_6)\langle S_1S_2S_3^2S_4^2\rangle \\ & +4(n_6-3n_4+3n_2-n_1)\langle S_1S_2^2S_3^2S_4^2\rangle \\ & +(p_0-4p_2+6p_3-4p_5+p_7)\langle S_1^2S_2^2S_3^2S_4^2\rangle\end{aligned}$$

$$\begin{aligned}\langle S_1S_0^2\rangle = {} & (4p_2-3p_0)\langle S_1\rangle + 4n_1\langle S_1^2\rangle + 6(p_0+p_1-2p_2+p_3)\langle S_1S_2^2\rangle \\ & +12(n_2-n_1)\langle S_1^2S_2^2\rangle + 4n_3\langle S_1S_2S_3^2\rangle \\ & +4(p_5+3p_4-3p_3+3p_2-3p_1-p_0)\langle S_1S_2^2S_3^2\rangle\end{aligned}$$

$$
\begin{aligned}
&+12(n_1-2n_2+n_4)\langle S_1^2S_2^2S_3^2\rangle\\
&+p_8\langle S_1S_2S_3S_4^2\rangle+4(n_5-n_3)\langle S_1S_2S_3^2S_4^2\rangle\\
&+(p_0+6p_1-4p_2+6p_3-12p_4-4p_5+6p_6+p_7)\langle S_1S_2^2S_3^2S_4^2\rangle\\
&+4(n_6-3n_4+3n_2-n_1)\langle S_1^2S_2^2S_3^2S_4^2\rangle\\
\langle S_1^2S_0^2\rangle &= 4n_1\langle S_1\rangle+(4p_2-3p_0)\langle S_1^2\rangle+12(n_2-n_1)\langle S_1S_2^2\rangle\\
&+6(p_0+p_1-2p_2+p_3)\langle S_1^2S_2^2\rangle+4(3n_1-6n_2+n_3+3n_4)\langle S_1S_2^2S_3^2\rangle\\
&+4(p_5+3p_4-3p_3+3p_2-3p_1-p_0)\langle S_1^2S_2^2S_3^2\rangle+p_8\langle S_1S_2S_3^2S_4^2\rangle\\
&+4(n_6+n_5-3n_4-n_3+3n_2-n_1)\langle S_1S_2^2S_3^2S_4^2\rangle\\
&+(p_0+6p_1-4p_2+6p_3-12p_4-4p_5+6p_6+p_7)\langle S_1^2S_2^2S_3^2S_4^2\rangle\\
\langle S_1S_2S_0^2\rangle &= (3p_0+6p_1-8p_2+6p_3)\langle S_1S_2\rangle+4(3n_2-2n_1)\langle S_1S_2^2\rangle\\
&+4(p_5+3p_4-3p_3+3p_2-3p_1-p_0)\langle S_1S_2S_3^2\rangle\\
&+4(3n_1-6n_2+n_3+3n_4)\langle S_1S_2^2S_3^2\rangle\\
&+(p_8+p_7+6p_6-4p_5-12p_4+6p_3-4p_2+6p_1+p_0)\langle S_1S_2S_3^2S_4^2\rangle\\
&+4(n_6+n_5-3n_4-n_3+3n_2-n_1)\langle S_1S_2^2S_3^2S_4^2\rangle\\
\langle S_1S_2^2S_0^2\rangle &= 4(3n_2-2n_1)\langle S_1S_2\rangle+(3p_0+6p_1-8p_2+6p_3)\langle S_1S_2^2\rangle\\
&+4(3n_1-6n_2+n_3+3n_4)\langle S_1S_2S_3^2\rangle\\
&+4(p_5+3p_4-3p_3+3p_2-3p_1-p_0)\langle S_1S_2^2S_3^2\rangle\\
&+4(n_6+n_5-3n_4-n_3+3n_2-n_1)\langle S_1S_2S_3^2S_4^2\rangle\\
&+(p_0+6p_1-4p_2+6p_3-12p_4-4p_5+6p_6+p_7+p_8)\langle S_1S_2^2S_3^2S_4^2\rangle\\
\langle S_1^2S_2^2S_0^2\rangle &= 4(3n_2-2n_1)\langle S_1S_2^2\rangle+(3p_0+6p_1-8p_2+6p_3)\langle S_1^2S_2^2\rangle\\
&+4(3n_1-6n_2+n_3+3n_4)\langle S_1S_2^2S_3^2\rangle\\
&+4(p_5+3p_4-3p_3+3p_2-3p_1-p_0)\langle S_1^2S_2^2S_3^2\rangle\\
&+4(n_6+n_5-3n_4-n_3+3n_2-n_1)\langle S_1S_2^2S_3^2S_4^2\rangle
\end{aligned}
$$

$$+(p_0+6p_1-4p_2+6p_3-12p_4-4p_5+6p_6+p_7+p_8)\langle S_1^2S_2^2S_3^2S_4^2\rangle$$

$$\langle S_1S_2S_3S_0^2\rangle = (4p_5+12p_4-6p_3+4p_2-6p_1-p_0)\langle S_1S_2S_3\rangle$$
$$+4(n_1-3n_2+n_3+3n_4)\langle S_1S_2S_3^2\rangle$$
$$+(p_0+6p_1-4p_2+6p_3-12p_4-4p_5+6p_6+p_7+p_8)\langle S_1S_2S_3S_4^2\rangle$$
$$+4(n_6+n_5-3n_4-n_3+3n_2-n_1)\langle S_1S_2S_3^2S_4^2\rangle$$

$$\langle S_1S_2S_3^2S_0^2\rangle = 4(n_1-3n_2+n_3+3n_4)\langle S_1S_2S_3\rangle$$
$$+(4p_5+12p_4-6p_3+4p_2-6p_1-p_0)\langle S_1S_2S_3^2\rangle$$
$$+4(n_6+n_5-3n_4-n_3+3n_2-n_1)\langle S_1S_2S_3S_4^2\rangle$$
$$+(p_0+6p_1-4p_2+6p_3-12p_4-4p_5+6p_6+p_7+p_8)\langle S_1S_2S_3^2S_4^2\rangle$$

$$\langle S_1S_2^2S_3^2S_0^2\rangle = 4(n_1-3n_2+n_3+3n_4)\langle S_1S_2S_3^2\rangle$$
$$+(4p_5+12p_4-6p_3+4p_2-6p_1-p_0)\langle S_1S_2^2S_3^2\rangle$$
$$+4(n_6+n_5-3n_4-n_3+3n_2-n_1)\langle S_1S_2S_3^2S_4^2\rangle$$
$$+(p_0+6p_1-4p_2+6p_3-12p_4-4p_5+6p_6+p_7+p_8)\langle S_1S_2^2S_3^2S_4^2\rangle$$

$$\langle S_1^2S_2^2S_3^2S_0^2\rangle = 4(n_1-3n_2+n_3+3n_4)\langle S_1S_2^2S_3^2\rangle$$
$$+(4p_5+12p_4-6p_3+4p_2-6p_1-p_0)\langle S_1^2S_2^2S_3^2\rangle$$
$$+4(n_6+n_5-3n_4-n_3+3n_2-n_1)\langle S_1S_2^2S_3^2S_4^2\rangle$$
$$+(p_0+6p_1-4p_2+6p_3-12p_4-4p_5+6p_6+p_7+p_8)\langle S_1^2S_2^2S_3^2S_4^2\rangle \quad (4.1.14)$$

If equation (4.1.14) is written in the form of a 34×34 matrix and solved in terms of the variables $x_i[(i=1,2,...,34)(e.g.,x_1=\langle S_0\rangle, x_2=\langle S_1S_0\rangle,...,x_{34}=\langle S_1^2S_2^2S_3^2S_0^2\rangle)]$ of the linear equations, all of the spin correlation functions can be determined easily as a function of the temperature, effective field, crystal field and the longitudinal magnetic field which other studies in the literature do not include. Since the thermal average of the central spin is equal to that of its

nearest-neighbor spins within the present method, the unknown parameter A can be determined numerically by the relation

$$\langle S_0 \rangle = \langle S_1 \rangle \qquad \text{or} \qquad x_1 = x_5 \tag{4.1.15}$$

By solving equation (4.1.15) numerically, at fixed values of D/J and h/J, we have obtained the parameter A. Then, we used the numerical values of A to obtain the spin correlation functions $\langle S_0 \rangle$, $\langle S_1 S_0 \rangle$, $\langle S_1 S_2 S_0 \rangle$, $\langle S_0^2 \rangle$ (quadrupole moment) and $\langle S_1^2 S_0^2 \rangle$ (biquadrupole moment) and so on, which can be found from equation (4.1.14). Note that $A = 0$ is always the root of the equation (4.1.15), corresponding to the disordered state of the system. The nonzero root of A in equation (4.1.15) corresponds to the long-range order state of the system.

4.2 Effective-Field Theory Analysis for the Blume-Capel Model

In this section, we present numerical results for the longitudinal magnetization, hysteresis loops, susceptibility, internal energy and specific heat of the spin-1 system with crystal-field in a longitudinal magnetic field, on the square lattice within the framework of the effective field with correlations. All of the spin correlation functions obtained from equation (4.1.14) are a function of temperature, exchange interaction, crystal-field and longitudinal magnetic field and depend on the value of temperature, longitudinal magnetic field and spin, respectively. If we insert the numerical values of A obtained from equation (4.1.15) at selected values of h/J for a fixed value of D/J into the spin correlation function $\langle S_0 \rangle$ obtained from equation (4.1.14), we can find the temperature dependence of $\langle S_0 \rangle$ (it is labeled as the longitudinal magnetization m, $(m_0 = m_1 = m)$) for the spin-1 system on the square lattice. By solving the self-consistent relation corresponding to equation (4.1.15) numerically for a fixed value of D/J at the selected values of h/J for the spin-1 system, we have obtained the numerical values of the parameter A. Then, by inserting the numerical values of A obtained from equation (4.1.15) at selected values of h/J for a fixed value of D/J into the spin correlation function $\langle S_0 \rangle$ obtained from equation (4.1.14), we have obtained

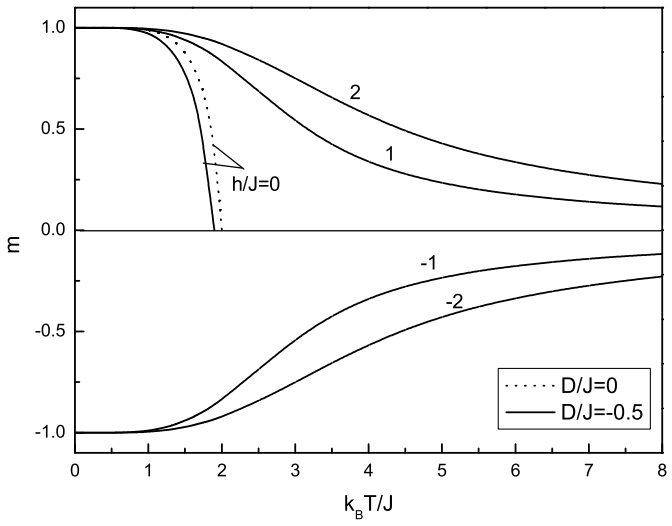

Figure 4.1 Magnetization versus temperature for spin-1 system with crystal field on a square lattice. The numbers accompanying each line are the values of the longitudinal magnetic field.

the temperature dependence of magnetization ($m = \langle S_0 \rangle$) on the square lattice. The numerical results are plotted in Fig. 4.1. The numbers on the curves are the values of longitudinal magnetic field. As shown in Fig. 4.1, in the case of $h/J = 0$, the longitudinal magnetization m falls rapidly from its saturation magnetization value ($m = 1.0$) to zero as temperature increases and, decreases continuously in the vicinity of transition temperature and vanishes at $T = T_c$; this is the second order phase transition. We clearly find that the transition temperature of the spin-1 system for fixed values of $D/J = 0$ and $h/J = 0$ is

$$k_B T_c/J = 1.964 \tag{4.2.1}$$

The critical temperature value in equation (4.2.1) is much closer to those obtained by the (EBPA) (Du et al, 2003) and the (BA) (Tanaka & Uryu, 1981) than those obtained by the (EFT) (Siqueira & Fittipaldi, 1986), (CEFT) (Kaneyoshi & Tamura, 1982; Honmura, 1984), a new type theory of cluster (Kaneyoshi, 1999a,b) and (DA) (Kaneyoshi, 2000), respectively. For comparison, the transition temperature $k_B T_c/J$ at $D/J = 0$ and $h/J = 0$ obtained by several methods and present work for spin-1 Ising system are given

in Table 4.1.

Table 4.1 Transition temperature k_BT_c/J at $D/J = 0$ and $h/J = 0$ obtained by several methods and present work.

MFA	SE	BA	EBPA	EFT	DA	Present Work
2.667	1.688	2.065	1.915	2.188	2.117	1.964

When we apply the longitudinal magnetic field ($h > 0$ or $h < 0$) to the system, the absolute value of magnetization decreases slowly from its saturation magnetization value as the temperature increases. This type of magnetization curves in the presence of an external magnetic field is not described in the Neel theory. The remaining magnetizations are getting bigger as the longitudinal magnetic field increases. From our calculation, we can see that the longitudinal magnetization curves are symmetric for both positive and negative longitudinal magnetic field. These results are in good agreement with those of previous works (Canpolat et al, 2007; Ekiz & Keskin, 2003; Ekiz, 2005; Jiang et al, 2005; Jiang & Bai, 2005, 2006; Mancini & Naddeo, 2006; Wei et al, 2004), but they are quite different from those of in references (Jiang & Wei, 2000; Jiang et al, 2000a, 2000b, 20001; Htoutou et al, 2004; Polat et al, 2003; Kaneyoshi, 1987, 1988; Kaneyoshi et al, 1992a; Bobak & Jurcisin, 1997) without applying longitudinal magnetic field.

We have also investigated the influence of longitudinal magnetic field h on the longitudinal magnetization process at the fixed values of temperature and crystal field for the spin-1 system with crystal field (Blume-Capel (BC)) model on the square lattice (Balcerzak, 2003). In order to present these hysteresis loops, we selected four typical temperatures and four crystal field parameter values in Fig. 4.2(a) and in Fig. 4.2(b), respectively. As we can see from Fig. 4.2(a) and Fig. 4.2(b), the details of the hysteresis loops depend on the temperature and the value of the crystal field. At fixed value of $D/J = -0.5$, the hysteresis loops of the square lattice for spin-1 system is shown in Fig. 4.2(a). From Fig. 4.2(a), we can see that the hysteresis loops do not occur at temperatures above the

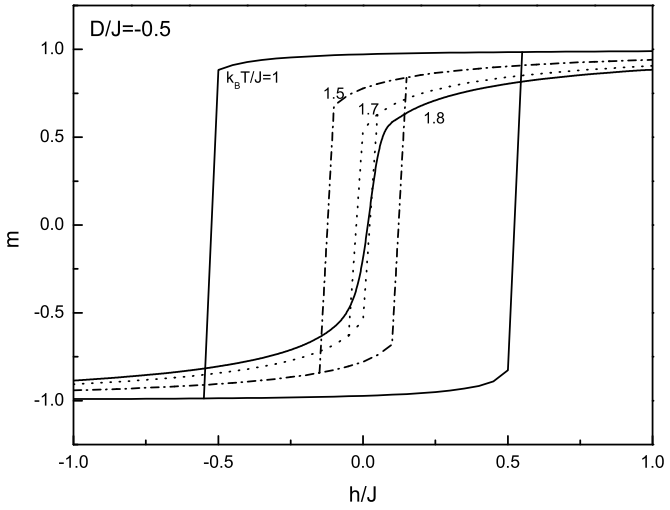

(a)

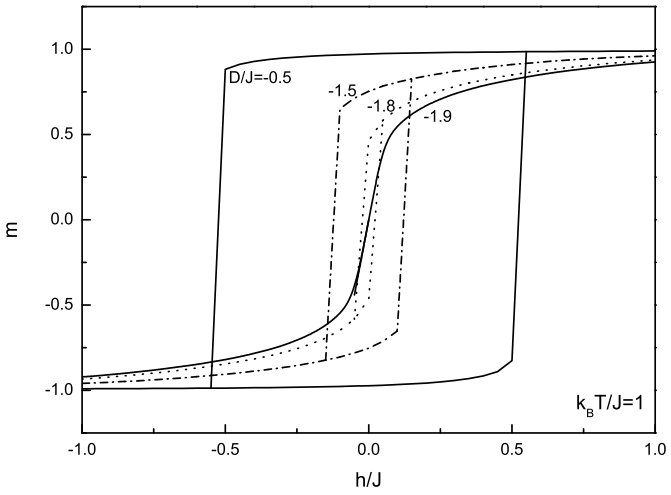

(b)

Figure 4.2 (a) The hysteresis loops for the spin-1 system when the crystal field is selected as $D/J = -0.5$ with four values of temperature k_BT/J . (b) The hysteresis loops for the spin-1 system when the temperature is selected as $k_BT/J = 1$ with four values of crystal field D/J.

critical temperature $k_BT_c/J = 1.8314$, called the Curie temperature, and the type of hysteresis loop becomes narrower with increasing temperature below the transition temperature. Then the hysteresis loop disappears when the temperature is higher than the transition temperature as in (Jiang et al, 2005; Jiang & Bai, 2005; Jiang & Bai, 2006). When the temperature is fixed as $k_BT/J = 1$, the hysteresis loops for the square lattice are plotted in Fig. 4.2(b). As seen from Fig. 4.2(b), the type of hysteresis loops becomes narrower with increasing the absolute value of the crystal field. Then the hysteresis loop disappears when the absolute value of the crystal field is large enough. Namely, these results are show that the hysteresis loops at low temperature are considered to originate from the competing effects of the interaction between the exchange interaction term of the nearest-neighbor pair of spins and the crystal field anisotropy and the Zeeman energy term in equation (4.1.1) of spin-1 system.

Now, we state how to calculate the thermodynamic parameters like susceptibility, internal energy and specific heat of spin-1 Blume-Capel model on the square lattice. The longitudinal susceptibility for the system which describes the characteristics of the change of magnetization with magnetic field and which can show the phase transition's properties, particularly its critical temperature can be determined from the relation

$$\chi = \frac{\partial \langle S_0 \rangle}{\partial h} \tag{4.2.2}$$

The internal energy U per site of the system can be obtained easily from the thermal average of the Hamiltonian in equation (4.1.1). Thus, the internal energy is given by

$$-\frac{U}{NJ} = q\langle S_0 S_1 \rangle + \frac{D}{J}\langle S_0^2 \rangle + \frac{h}{J}\langle S_0 \rangle \tag{4.2.3}$$

where the correlation functions $\langle S_0 \rangle$, $\langle S_0^2 \rangle$ and $\langle S_1 S_0 \rangle$ are obtained easily from equation (4.1.14) for spin-1 system. With the use of equation (4.2.3), the specific heat of the system can be determined from the relation

$$C_h = \left(\frac{\partial U}{\partial T} \right)_h \tag{4.2.4}$$

In order to illustrate the theoretical results numerically, we have performed analysis for the spin-1 system on the square lattice. Thermodynamic quantities are plotted in Figs. 4.3-4.6 as a function of dimensionless temperature k_BT/J.

In Fig. 4.3(a), we have given numerical results of the susceptibility for spin-1 system on the square lattice in the $(\chi, k_BT/J)$ plane for the selected values of $h/J = 0$, 0.1, 0.5 when the crystal field is selected as $D/J = 0, -0.5$. Our results are in good agreement with those of previous works (Wei et al, 2004; Jiang et al, 2005; Jiang & Bai, 2005; Jiang & Bai, 2006; Du et al, 2004; Mancini & Naddeo, 2006; Balcerzak, 2003; Canpolat et al, 2007). From Fig. 4.3(a), we can clearly see a peak at the critical temperature that corresponds to the divergence of the longitudinal susceptibility for $h/J = 0$. Furthermore, as seen from the figures, in the absence of the longitudinal magnetic field ($h/J = 0$), the curve of susceptibility rapidly increases and expresses a peak at the phase transition temperature and then rapidly decreases as the temperature increases. In the presence of a longitudinal magnetic field, the phase transition is not observed, and the stronger the longitudinal magnetic field, the smaller is the susceptibility, reflecting the fact that the longitudinal magnetization is weaker. In Fig. 4.3(b), the longitudinal susceptibility is plotted in the absence of longitudinal magnetic field ($h = 0$) with selected values of $D/J = 0, -0.5, -1, -1.5$. We can clearly see from Fig. 4.3(b) that the critical temperature value k_BT_c/J decreases as the absolute value of crystal field increases, and critical temperature has a double valued form for $D < -1$, (see Fig.7.1).

In Figs. 4.4-4.6, the temperature dependencies of the internal energy U and specific heat C are plotted for spin-1 system. Using the numerical derivative of the internal energy with respect to temperature, we obtain the behavior of the specific heat with temperature and the anisotropy parameter. These quantities for spin-1 system with crystal field on honeycomb lattice ($q = 3$) are studied in (Canpolat et al, 2007). We can see that from Fig. 4.4(a), for the selected four values of h/J, if the longitudinal magnetic field increases, then the absolute value of internal energy increases. In the case of $h/J = 0$, the specific heat curve of spin-1 system in Fig. 4.4(b) exhibits a second order phase transition at the Curie temperature

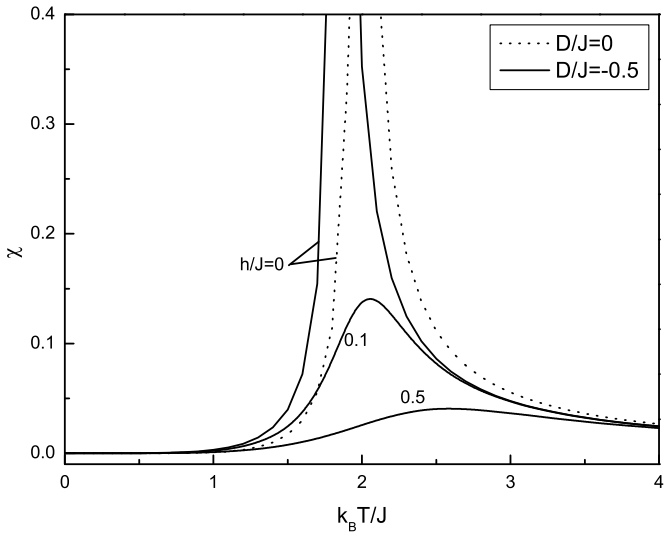

(a)

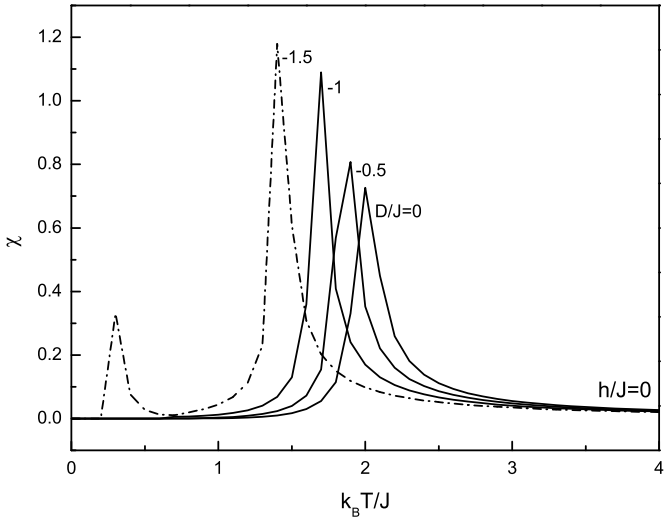

(b)

Figure 4.3 (a) The susceptibility for the spin-1 system when the crystal field is selected as $D/J = 0, -0.5$. The numbers on the each curve are the values of longitudinal magnetic field h/J. (b) The susceptibility for the spin-1 Ising system when the longitudinal magnetic field is selected as $h/J = 0$. The numbers on the each curve are the values of the crystal field D/J.

$k_BT/J = 1.9$ and rapidly decreases with increasing temperature. In the case of $h/J \neq 0$, the phase transition has also been removed and, we see that the derivatives of internal energy are flattened with increasing external field. Next, in the cases of $h/J = 0$ and $h/J \neq 0$, we have plotted the temperature dependencies of the internal energy U and specific heat C for spin-1 system on the square lattice at selected values of D/J. In the case of $h/J = 0$ the behavior of internal energy with temperature and crystal field parameter is shown in figure Fig. 4.5(a) at fixed values of $D/J = -1.901, -1, -0.5, 0$. The internal energy decreases suddenly at the transition temperature as the crystal field parameter D/J gets just $D_t/J = -1.901$ in the negative direction, which is similar to that in (Siqueira & Fittipaldi, 1986). The tricritical point is such a point that, at which the system shows from the second-order to the first-order phase transition in the Ising system. We can interpret it as the fact that the spin-1 Ising system (or BC model) exhibits a first-order transition at a negative tricritical value D_t/J such that $D_t/J = -1.901$ for $q = 4$. For four selected values of the crystal field D/J, the specific heat C curves of the spin-1 system exhibit second-order phase transition at the Curie temperature. As expected, the transition temperatures of C/Nk_B increase as the crystal field strength increases, (Fig. 4.5(b)). However, when D/J becomes smaller than $D/J = -1$, the discontinuity character of specific heat begins to increase in height. When the crystal field gets just to the value of the tricritical point, a jumping appears in the specific heat curve at the transition point and the transition point increases in height (as inset in the Fig. 4.5(b)). This behavior can be interpreted as a competition between the exchange interaction which tries to align the spins in the same direction, and the effect of the crystal field anisotropy which has the tendency to destroy this alignment in the considered system.

In the case of $h/J \neq 0$, our results do not have a discontinuity behavior or phase transition point at all values of D/J. Fig. 4.6(a) curves have a continuous form and the absolute value of internal energy increases with increasing values of D/J . It is seen from Fig. 4.6(b) that the specific heat curves have a relatively maximum-like Schottky peak at a certain value of the temperature and the height of the specific heat peak increases with increasing values of D/J and moves towards

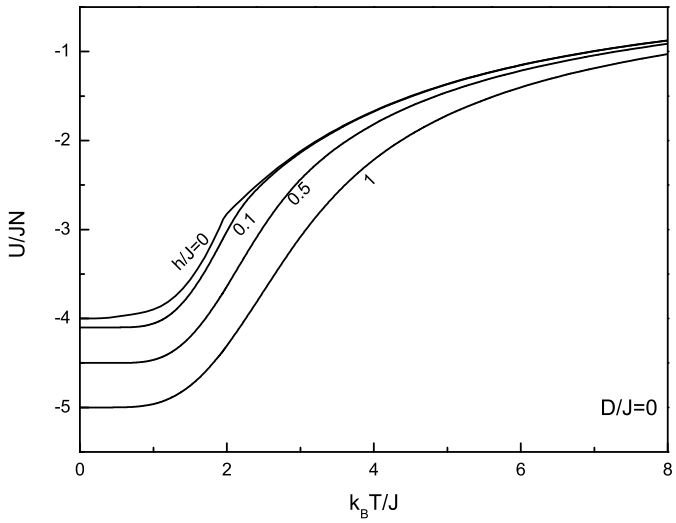

(a)

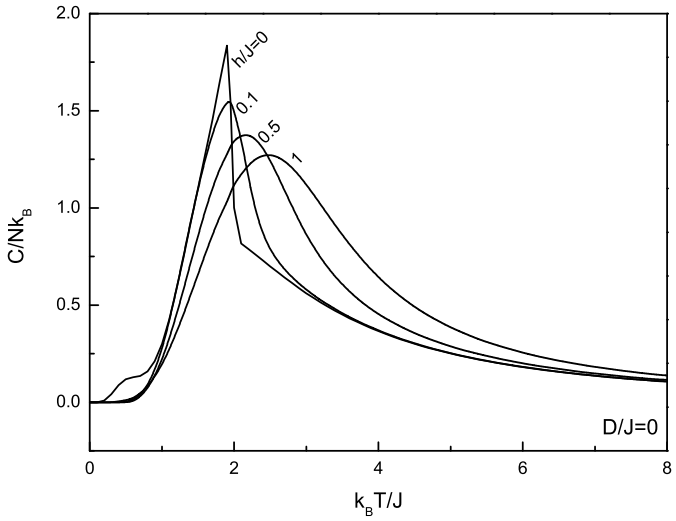

(b)

Figure 4.4 The temperature dependence of (a) the internal energy U and (b) the specific heat C for the spin-1 Ising model on a square lattice when the crystal field is selected as D/J=0 at selected values of h/J= 0, 0.1, 0.5 and 1.

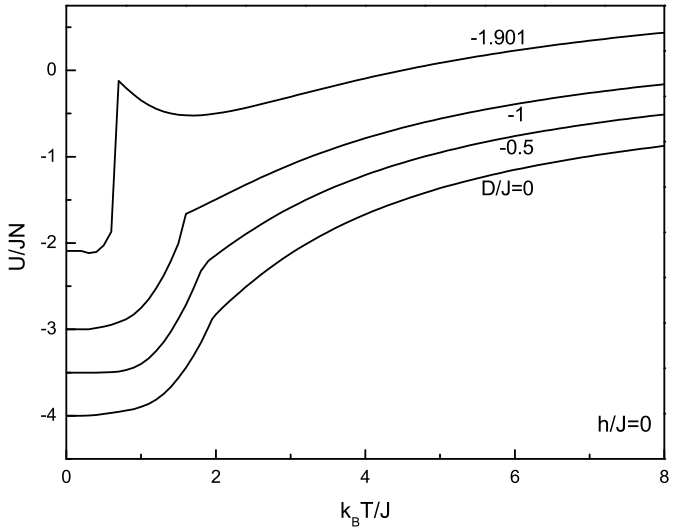

(a)

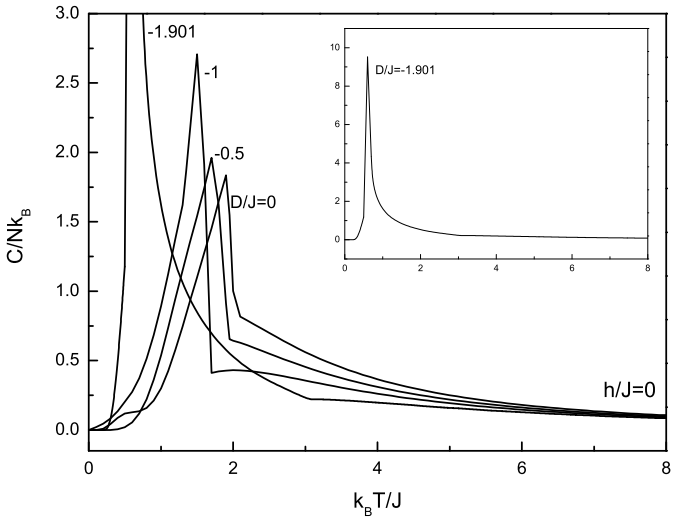

(b)

Figure 4.5 The temperature dependence of (a) the internal energy U and (b) the specific heat C for the spin-1 Ising model on a square lattice when the longitudinal magnetic field is selected as h/J=0 at selected values of D/J = -1.901, -1, -0.5 and 0.

increasing temperature when the crystal field D/J increases. We note that the Schottky-like round hump in the specific heat probably reflects the fact that the energy of the system depends on the longitudinal magnetic field h/J and the crystal field D/J. However, they do not indicate that a second-order phase transition occurs in the 2D system. In the case of $h/J \neq 0$, all of them may be thought of as Schottky-like peaks resulting from the ferromagnetic short-range order.

The shapes of the internal energy and specific heat curves qualitatively agree with those obtained by the various methods (Mancini & Naddeo, 2006; Balcerzak, 2003; Siqueira & Fittipaldi, 1986; Kaneyoshi & Jascur, 1992; Micnas, 1979; Ng & Barry, 1978; Du et al, 2003). As a result, by comparing the curves for nonzero values of h/J, we see that the phase transition has been removed in the system. According to us, it is originated from the presence of external magnetic field in the system. All calculated properties show the proper thermodynamical behavior over the whole range of temperatures, including the ground state behavior ($\chi \to 0$ and $C \to 0$ for $T \to 0$) and the thermal stability condition ($C_h \geq 0$).

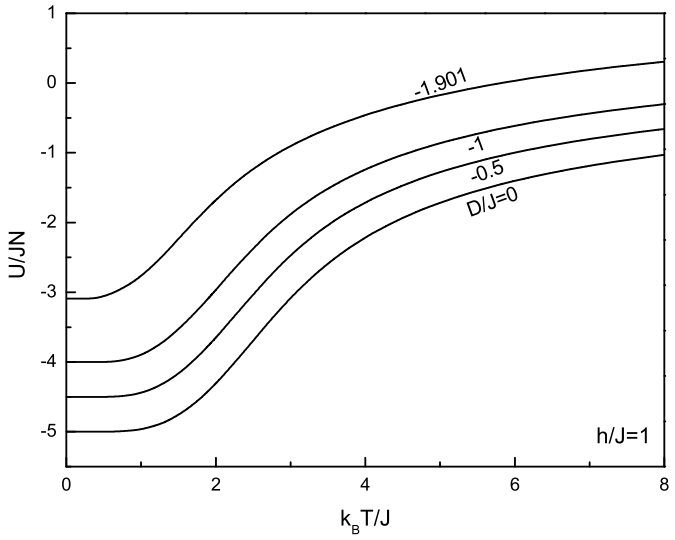

(a)

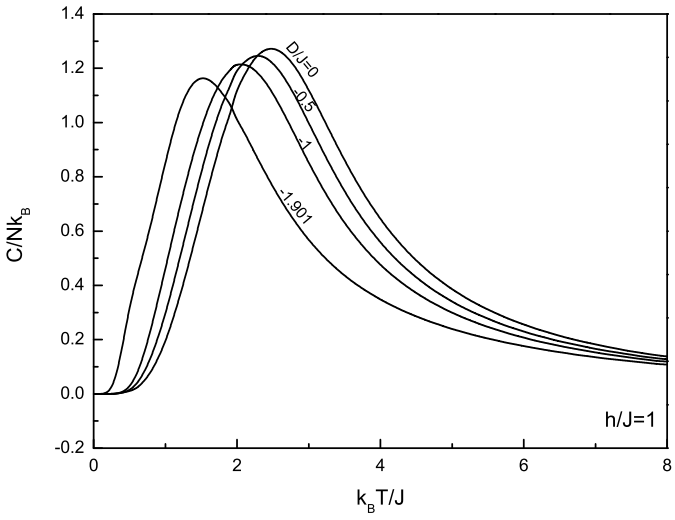

(b)

Figure 4.6 The temperature dependence of (a) the internal energy U and (b) the specific heat C for the spin-1 Ising model on a square lattice when the longitudinal magnetic field is selected as h/J=1 at selected four negative values of D/J=-1.901, -1, -0.5 and 0.

CHAPTER FIVE
CANONICAL ENSEMBLE AND MONTE CARLO SIMULATION

5.1 Canonical ensemble

Most physical systems are not isolated, but exchange energy with their environment. Because such systems are usually small in comparison to their environment, we assume that any change in the energy of the smaller system does not have a significant effect on the temperature of the environment. We say that the environment acts as a *heat reservoir* or *heat bath* at a fixed absolute temperature T. If a small but macroscopic system is placed in thermal contact with a heat bath, the system reaches thermal equilibrium by exchanging energy with the heat bath until the system attains the temperature of the bath.

Imagine an infinitely large number of copies of a system at fixed volume V and number of particles N in equilibrium at temperature T. P_s, the probability that the system is in microstate s with energy E_s, is given by

$$P_s = \frac{1}{Z} e^{-\beta E_s} \qquad \text{(canonical distribution)} \qquad (5.1.1)$$

where $\beta = 1/k_B T$, and Z is a normalization constant. The ensemble defined by (5.1.1) is known as the *canonical* ensemble. Because $\sum P_s = 1$, and Z is given by

$$Z = \sum_{s=1}^{M} e^{-E_s/k_B T} \qquad (5.1.2)$$

The summation in (5.1.2) is over all M accessible microstates of the system. The quantity Z is known as the *partition function* of the system. We can use (5.1.1) to obtain the ensemble average of the physical quantities of interest. For example, the mean energy is given by

$$\langle E \rangle = \sum_{s=1}^{M} E_s P_s = \frac{1}{Z} \sum_{s=1}^{M} E_s e^{-\beta E_s} \qquad (5.1.3)$$

Note that energy fluctuates in the canonical ensemble, (Gould & Tobochnik, 1996).

5.2 Fluctuations in the Canonical Ensemble

We first obtain the relation of the constant volume heat capacity C_V to the energy fluctuations in the canonical ensemble. We adopt the notation $U = \langle E \rangle$ and write C_V as

$$C_V = \frac{\partial U}{\partial T} = -\frac{1}{k_B T^2} \frac{\partial U}{\partial \beta} \tag{5.2.1}$$

From (5.1.3) we have

$$U = -\frac{\partial}{\partial \beta} \ln Z \tag{5.2.2}$$

and

$$\begin{aligned} \frac{\partial U}{\partial \beta} &= -\frac{1}{Z^2} \frac{\partial Z}{\partial \beta} \sum_s E_s e^{-\beta E_s} - \frac{1}{Z} \sum_s E_s^2 e^{-\beta E_s} \\ &= \langle E \rangle^2 - \langle E^2 \rangle \end{aligned} \tag{5.2.3}$$

using the relations (5.2.1) and (5.2.3) one obtains the relation

$$C_V = \frac{1}{k_B T^2} \left(\langle E^2 \rangle - \langle E \rangle^2 \right) \tag{5.2.4}$$

Note that the heat capacity is at constant volume because the partial derivatives were performed with the energy levels E_s kept constant. The corresponding quantity for a magnetic system is the heat capacity at constant external magnetic field.

The relation of the magnetic susceptibility χ to the fluctuations of the magnetization m can be obtained in a similar way. We assume that the energy

can be written as

$$E_s = E_{0,s} - hm_s \tag{5.2.5}$$

where $E_{0,s}$ is the energy in the absence of a magnetic field, h is the external applied field, and m_s is the magnetization in the s state. The mean magnetization is given by

$$\langle m \rangle = \frac{1}{Z} \sum m_s e^{-\beta E_s} \tag{5.2.6}$$

Because $\partial E_s / \partial h = -m_s$, we have

$$\frac{\partial Z}{\partial h} = \sum_s \beta m_s e^{-\beta E_s} \tag{5.2.7}$$

Hence we obtain

$$\langle m \rangle = \frac{1}{\beta} \frac{\partial}{\partial h} \ln Z \tag{5.2.8}$$

If we use (5.2.6) and (5.2.8), we find

$$\frac{\partial \langle m \rangle}{\partial h} = -\frac{1}{Z^2} \frac{\partial Z}{\partial h} \sum_s m_s e^{-\beta E_s} + \frac{1}{Z} \sum_s \beta m_s^2 e^{-\beta E_s}$$

$$= -\beta \langle m \rangle^2 + \beta \langle m^2 \rangle \tag{5.2.9}$$

Definition of the magnetic susceptibility which is thermodynamic derivative of mean magnetization is

$$\chi = \lim_{h \to 0} \frac{\partial \langle m \rangle}{\partial h} \tag{5.2.10}$$

By using the relations (5.2.10) and (5.2.9) the zero field susceptibility can be obtained as

$$\chi = \frac{1}{k_B T} \left(\langle m^2 \rangle - \langle m \rangle^2 \right) \tag{5.2.11}$$

5.3 What is a Monte Carlo Simulation?

In a Monte Carlo simulation we attempt to follow the "time dependence" of a model for which change, or growth, does not proceed in some rigorously predefined fashion (e.g. according to Newton's equations of motion) but rather in a stochastic manner which depends on a sequence of random numbers which is generated during the simulation. With a second, different sequence of random numbers the simulation will not give identical results but will yield values which agree with those obtained from the first sequence to within some "statistical error". A very large number of different problems fall into this category: in percolation an empty lattice is gradually filled with particles by placing a particle on the lattice randomly with each "tick of the clock". Lots of questions may then be asked about the resulting "clusters" which are formed of neighboring occupied sites. Particular attention has been paid to the determination of the "percolation threshold", i.e. the critical concentration of occupied sites for which an "infinite percolating cluster" first appears. A percolating cluster is one which reaches from one boundary of a (macroscopic) system to the opposite one. The properties of such objects are of interest in the context of diverse physical problems such as conductivity of random mixtures, flow through porous rocks, behavior of dilute magnets, etc. Another example is diffusion limited aggregation (DLA) where a particle executes a random walk in space, taking one step at each time interval, until it encounters a "seed" mass and sticks to it. The growth of this mass may then be studied as many random walkers are turned loose. The "fractal" properties of the resulting object are of real interest, and while there is no accepted analytical theory of DLA to date, computer simulation is the method of choice. In fact, the phenomenon of DLA was first discovered by Monte Carlo simulation.

Considering problems of statistical mechanics, we may be attempting to sample a region of phase space in order to estimate certain properties of the model, although we may not be moving in phase space along the same path which an exact solution to the time dependence of the model would yield. Remember that the task of equilibrium statistical mechanics is to calculate thermal averages of

(interacting) many-particle systems: Monte Carlo simulations can do that, taking proper account of statistical fluctuations and their effects in such systems. Since the accuracy of a Monte Carlo estimate depends upon the thoroughness with which phase space is probed, improvement may be obtained by simply running the calculation a little longer to increase the number of samples. Unlike in the application of many analytic techniques (e.g. perturbation theory for which the extension to higher order may be prohibitively difficult), the improvement of the accuracy of Monte Carlo results is possible not just in principle but also in practice, (Landau & Binder, 2000).

5.4 Metropolis Algorithm

How can we simulate a system of N particles confined in a volume V at a fixed temperature T? Because we can generate only a finite number m of the total number of M microstates, we might hope to obtain an estimate for the mean value of the physical quantity A by writing

$$\langle A \rangle \approx A_m = \frac{\sum_{s=1}^{m} A_s e^{-\beta E_s}}{\sum_{s=1}^{m} e^{-\beta E_s}} \tag{5.4.1}$$

A_s is the volume of the physical quantity A in the microstate s. A crude Monte Carlo procedure is to generate a microstate s at random, calculate E_s, A_s, and $e^{-\beta E_s}$, and evaluate the corresponding contribution of the microstate to the sums in (5.4.1). However, a microstate generated in this way would likely be very improbable and hence contribute little to the sums. Instead, we use an importance sampling method and generate microstates according to a probability distribution function π_s.

We rewrite (5.4.1) by multiplying and dividing by π_s.

$$A_m = \frac{\sum_{s=1}^{m} (A_s/\pi_s) e^{-\beta E_s} \pi_s}{\sum_{s=1}^{m} (1/\pi_s) e^{-\beta E_s} \pi_s} \qquad \text{no importance sampling} \tag{5.4.2}$$

If we generate microstates with probability π_s, then (5.4.2) becomes

$$A_m = \frac{\sum_{s=1}^{m}(A_s/\pi_s)e^{-\beta E_s}}{\sum_{s=1}^{m}(1/\pi_s)e^{-\beta E_s}} \qquad \text{importance sampling} \tag{5.4.3}$$

That is, if we average over a biased sample, we need to weight each microstate by $1/\pi_s$ to eliminate the bias. Although any form of $1/\pi_s$ could be used, the form of (5.4.3) suggests that a reasonable choice of $1/\pi_s$ is the Boltzmann probability itself, i.e.,

$$\pi_s = \frac{e^{-\beta E_s}}{\sum_{s=1}^{m} e^{-\beta E_s}} \tag{5.4.4}$$

This choice of π_s implies that the estimate A_m of the mean value of A can be written as

$$A_m = \frac{1}{m}\sum_{s=1}^{m} A_s \tag{5.4.5}$$

The choice (5.4.4) for π_s is due to Metropolis et al.

The Metropolis algorithm can be summarized in the context of the simulation of a system of spins or particles as follows:

1. Establish an initial microstate.
2. Make a random trial change in the microstate. For example, choose a spin at random and flip it. Or choose a particle at random and displace it a random distance.
3. Compute $\triangle E \equiv E_{\text{trial}} - E_{\text{old}}$, the change in the energy of the system due to the trial change.
4. If $\triangle E$ is less than or equal to zero, accept the new microstate and go to step 8.
5. If $\triangle E$ is positive, compute the quantity $w = e^{-\beta \triangle E}$.
6. Generate a random number r in the unit interval.
7. If $r \leq w$, accept the new microstate; otherwise retain the previous microstate.

8. Determine the value of the desired physical quantities.

9. Repeat steps (2) through (8) to obtain a sufficient number of microstates.

10. Periodically compute averages over microstates.

Steps (2) through (7) give the conditional probability that the system is in microstate $\{S_j\}$ given that it was in microstate $\{S_i\}$. These steps are equivalent to the transition probability

$$W(i \to j) = \min(1, e^{-\beta \triangle E}), \qquad \text{(Metropolis algorithm)} \tag{5.4.6}$$

where $\triangle E = E_j - E_i$. $W(i \to j)$ is the probability per unit time for the system to make a transition from microstate i to microstate j. Because it is necessary to evaluate only the ratio $P_j/P_i = e^{-\beta \triangle E}$, it is not necessary to normalize the probability. Note that because the microstates are generated with a probability proportional to the desired probability, all averages become arithmetic averages as in (5.4.5). However, because the constant proportionality is not known, it is not possible to estimate the partition function Z in this way.

Although we choose π_s to be the Boltzmann distribution, other choices of π_s are possible and are useful in some contexts. In addition, the choice (5.4.6) of the transition probability is not the only one that leads to the Boltzmann distribution. It can be shown that if W satisfies the *detailed balance* condition

$$W(i \to j)e^{-\beta E_i} = W(j \to i)e^{-\beta E_j} \qquad \text{(detailed balance)} \tag{5.4.7}$$

then the corresponding Monte Carlo algorithm generates a sequence of states distributed according to the Boltzmann distribution. The derivation that the Metropolis algorithm generates states with a probability proportional to the Boltzmann probability distribution after a sufficient number of steps does not add much to our physical understanding of the algorithm.

We have implicitly assumed in the above discussion that the system is ergodic.

Ergodicity refers to the sampling of the important microstates of a system. In a Monte Carlo simulation, the existence of ergodicity depends on the way the trial moves are made, and on the nature of the energy barriers between microstates. For example, consider a one-dimensional lattice of Ising spins with all spins up. If the spins are updated sequentially from right to left, then if one spin is flipped, all remaining flips will be accepted regardless of the temperature because the change in energy is zero. Clearly, the system is not ergodic for this implementation of the algorithm, and we would not obtain the correct thermodynamic behavior, (Gould & Tobochnik, 1996).

5.5 Exact Enumeration of the 2x2 Ising Model

In general, a Monte Carlo simulation yields exact answers only after an infinite number of configurations have been sampled. For sufficiently small lattices, thermal averages may be obtained exactly and easily by direct enumeration. Because the number of possible states or configurations of the Ising model increases as 2^N, we can enumerate the possible configurations only for small N. As an example, we calculate the various quantities of interest for a 2×2 Ising model on the square lattice with periodic boundary conditions. In Table 5.1, we group the sixteen states according to their total energy and magnetization.

Table 5.1 The energy and magnetization of the 2^4 states of the zero field spin-1/2 Ising model on the 2×2 square lattice. The degeneracy is the number of microstates with the same energy.

Number spins up	Degeneracy	Energy	Magnetization
4	1	-8	4
3	4	0	2
2	4	0	0
2	2	8	0
1	4	0	-2
0	1	-8	-4

We can compute all the quantities of interest using Table 5.1. The partition

function is given by

$$Z = 2e^{8\beta J} + 12 + 2e^{-8\beta J} \tag{5.5.1}$$

If we use (5.2.2) and (5.5.1), we find

$$U = -\frac{\partial}{\partial \beta} \ln Z = -\frac{1}{Z}[16e^{8\beta J} - 16e^{-8\beta J}] \tag{5.5.2}$$

And the mean absolute magnetization is given by

$$\langle |M| \rangle = \frac{1}{Z}[8e^{8\beta J} + 16] \tag{5.5.3}$$

In order to test our program we compared our MC data for spin-1/2 system with the exact relations (5.5.2) and (5.5.3). The results are given in the table below. From the table we can see that our results are statistically meaningful.

Table 5.2 The comparison of energy and magnetization of simulation with the exact results.

Energy (exact)	Energy (simulation)	Magnetization (exact)	Magnetization (simulation)	Temperature
-2.0	-2.0	1.0	1.0	0.25
-1.99972	-1.9998	0.99991	0.9999	0.75
-1.94361	-1.9440	0.98121	0.9811	1.5
-1.80083	-1.8014	0.93371	0.9334	2.0
-1.60217	-1.6055	0.86783	0.8676	2.5
-1.39995	-1.4009	0.80111	0.8003	3.0

CHAPTER SIX
MONTE CARLO SIMULATION RESULTS

6.1 Monte Carlo Simulation Results for Blume-Emery-Griffiths Model

In this section, we present numerical results for the longitudinal magnetization, hysteresis loops, susceptibility, internal energy and specific heat of the spin-1 system with crystal-field in a longitudinal magnetic field, on the square lattice within the framework of the Monte Carlo Simulation technique and we compare our results with those of effective-field theory with correlations given in Section 4.2 for a special case of $K = 0$.

In addition to the bilinear exchange interaction J and single-ion anisotropy D of the standard Ising model, the spin-1 Ising model possesses a biquadratic exchange interaction K (Rachadi & Benyoussef, 2004). It is also known as the Blume-Emery-Griffiths (BEG) model (Blume & Emery & Griffiths, 1971) and the model with vanishing biquadratic interaction ($K = 0$) is known as the Blume-Capel (BC) model (Blume, 1966; Capel, 1966). The BEG model is described by the following Hamiltonian:

$$H = -J \sum_{<i,j>} S_i^z S_j^z - D \sum_i (S_i^z)^2 - K \sum_{<i,j>} (S_i^z)^2 \left(S_j^z\right)^2 - h \sum_i S_i^z \qquad (6.1.1)$$

where $S_i = 0, +1$ or -1 is the spin at site i and $\sum_{<ij>}$ stands for a summation over all nearest-neighbor pairs. A ferromagnetic interaction $J > 0$ is assumed between the nearest-neighbor spins and we set $J = 1$. We employed standard importance sampling methods to simulate the system described by the Hamiltonian in equation (6.1.1) on a $L \times L$ square lattice with periodic boundary conditions and data were obtained with $L = 16$. Configurations were generated by selecting the sites in sequence through the lattice and making single-spin-flip attempts, which were accepted or rejected according to the Metropolis algorithm. Data were generated with 25000 Monte Carlo steps per site after discarding the first

2500 steps. 10 independent MC runs of 25000 MC steps per spin have been performed at each temperature.

Now we can clarify how to calculate the thermodynamic parameters like longitudinal magnetization, susceptibility, internal energy and specific heat of spin-1 Blume-Emery-Griffiths model with $q = 4$. The longitudinal magnetization per spin is a sum over each spin on the lattice and it can be determined from the relation

$$m = \frac{1}{N} \sum_{i=1}^{N} S_i^z \tag{6.1.2}$$

and the relation of the magnetic susceptibility to the fluctuations of the magnetization can be written with the help of equation (6.1.2) as

$$\chi = \frac{\langle m^2 \rangle - \langle m \rangle^2}{k_B T} \tag{6.1.3}$$

The internal energy U per site of the system can be obtained easily by computing the average energy of each spin on the lattice. Thus, the internal energy of the BEG model is the average of the Hamiltonian in equation (6.1.1).

$$U = \frac{1}{L^2} \langle H \rangle \tag{6.1.4}$$

and lastly the specific heat of the system can be determined from the relation

$$C_h = \left(\frac{\partial U}{\partial T} \right)_h \tag{6.1.5}$$

where T and N denotes the temperature and the number of spins on the lattice, respectively.

Monte Carlo simulation results for spin-1 Ising model with biquadratic nearest-neighbor pair interaction (or BEG model) which is described by Hamiltonian (6.1.1) are as follow: Firstly, the temperature dependence of longitudinal magnetization m for the values of $K/J = 0$ and $D/J = 0$ can be seen in Fig. 6.1(a). The numbers on the curves are the values of longitudinal magnetic field. As shown in Fig. 6.1(a), in the case of $h/J = 0$, the longitudinal magnetization m

falls rapidly from its saturation magnetization ($m = 1.0$) to zero with increasing temperature and decreases continuously in the vicinity of transition temperature and vanishes at $T = T_c$; this is the second order phase transition. In order to locate the transition temperature of the system we computed the fourth order cumulant of magnetization $V_L(L,T)$ with various lattice sizes $L = 8$, 16, 32, 64. The fourth order cumulant of the magnetization, i.e. the Binder cumulant, for a spin cluster is defined by (Binder, 1981),

$$V_L(L,T) = 1 - \frac{\langle M^4 \rangle}{3\langle M^2 \rangle^2} \tag{6.1.6}$$

where $\langle M^2 \rangle$ and $\langle M^4 \rangle$ denote the second and fourth moments of the magnetization in that cluster, taking thermal averages. The cumulant approaches in the thermodynamic limit the value 2/3 at temperatures $T < T_c$, while it tends to zero, reflecting a Gaussian distribution of the magnetization histogram, at $T > T_c$ (Binder, 1981). At T_c, $V_L(L,T) = V_L^*$ acquires a nontrivial value, the critical Binder cumulant. The crossing point of the curves with $L = 8$, 16, 32, 64 gives us the transition temperature k_BT_c/J which is shown by a white circle in Fig. 6.1(b). We clearly find by using equation (6.1.6) that the transition temperature of the spin-1 BC model for fixed values of $D/J = 0$, $K/J = 0$ and $h/J = 0$ is

$$k_BT_c/J = 1.69 \tag{6.1.7}$$

This result is much closer to those obtained by series expansion (SE) analysis (Fox & Guttman, 1973; Adler & Enting, 1984; Blote & Nightingale, 1985) but it is clearly different from that we obtained within the framework of the effective-field theory with correlations. For comparison, the transition temperature k_BT_c/J at $D/J = 0$, $K/J = 0$, and $h/J = 0$ obtained by several methods and our MC simulations for spin-1 Ising system are given in Table 6.1.

Table 6.1 Transition temperature k_BT_c/J at $D/J = 0$ and $h/J = 0$ obtained by several methods and present work (MC).

MFA	SE	BA	EBPA	EFT	DA	MC
2.667	1.688	2.065	1.915	2.188	2.117	1.69

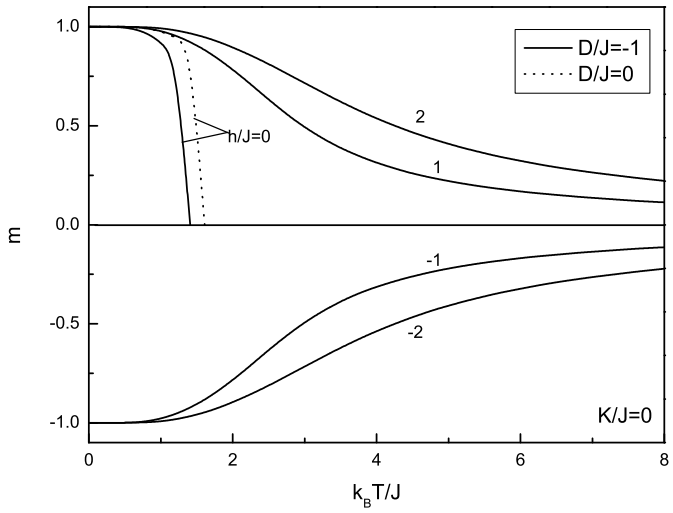

(a)

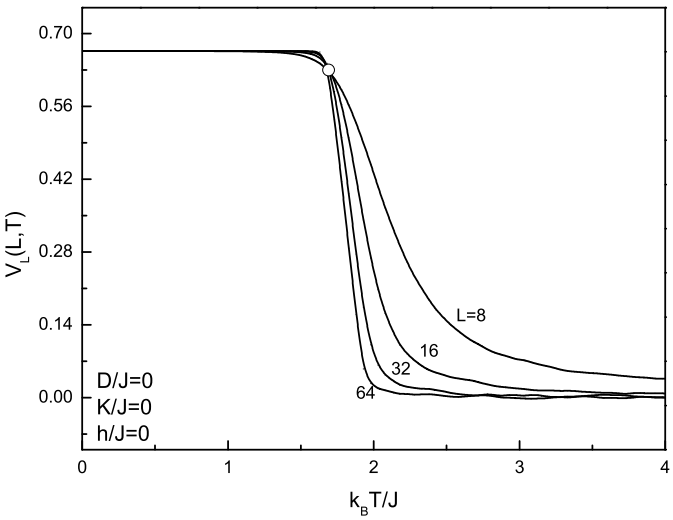

(b)

Figure 6.1 (a) Temperature dependence of magnetization for spin-1 system with crystal field on a square lattice. The numbers accompanying each line are the values of the longitudinal magnetic field. (b) Temperature dependence of fourth order magnetization cumulant V_L for $L = 8$, $L = 16$, $L = 32$, $L = 64$. White circle on the crossing point of the curves denotes the transition temperature.

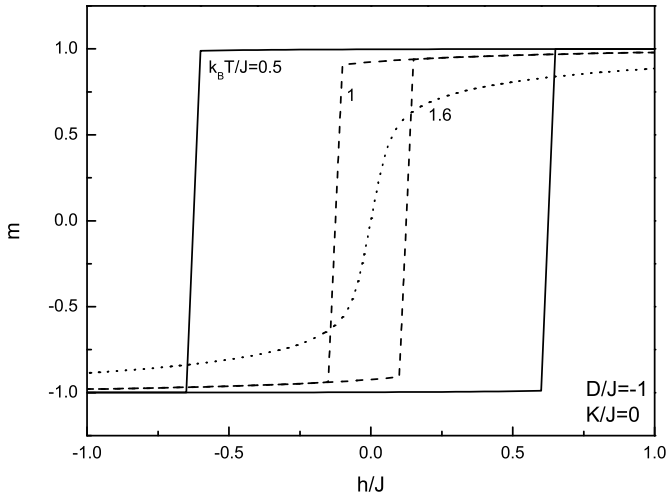

(a)

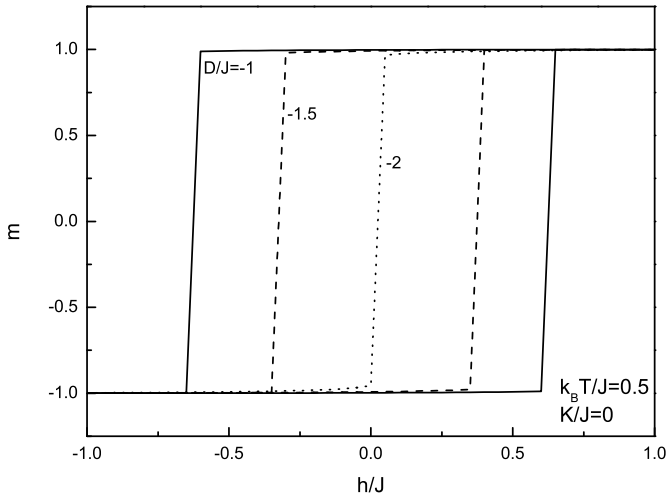

(b)

Figure 6.2 (a) The hysteresis loops for a square lattice of spin-1 system when the crystal field is selected as $D/J = -1$ with three values of temperature k_BT/J. (b) The hysteresis loops for the square lattice of spin-1 system when the temperature is selected as $k_BT/J = 0.5$ with three values of crystal field D/J.

In Fig. 6.2, we show that the influence of longitudinal magnetic field h on the longitudinal magnetization process at the fixed values of temperature and crystal field for the spin-1 Blume-Emery-Griffiths model on a square lattice. We selected

three typical temperatures and three crystal field parameter values in Fig. 6.2(a) and in Fig. 6.2(b), respectively. As we can see from Fig. 6.2(a) and Fig. 6.2(b), the details of the hysteresis loops depend on the temperature and the value of the crystal field. At fixed value of $D/J = -1$, the hysteresis loops of the spin-1 system on the square lattice is shown in Fig. 6.2(a). From Fig. 6.2(a), we can see that the hysteresis loops do not occur at temperatures above the critical temperature $k_BT_c/J = 1.26$, and the type of hysteresis loop becomes narrower as the temperature increases below the transition temperature. Then the hysteresis loop disappears when the temperature is higher than the transition temperature as in Fig. 4.2(a). When the temperature is fixed as $k_BT/J = 0.5$, the hysteresis loops for the square lattice are plotted in Fig. 6.2(b). As it is seen from Fig. 6.2(b), the type of hysteresis loops becomes narrower with increasing the absolute value of the crystal field. Then the hysteresis loop disappears when the absolute value of the crystal field is large enough. This behavior of hysteresis loops also agrees with those plotted in Fig. 4.2(b). In our simulations we found that in contrast to the temperature k_BT/J and single-ion anisotropy D/J, biquadratic exchange interaction K/J does not play a role on the type of hysteresis loop.

In Fig. 6.3(a), we have given numerical results of the susceptibility for spin-1 BEG model on a square lattice in the $(\chi, k_BT/J)$ plane for the selected values of $h/J = 0$, 0.1, 0.5, and 1 when the crystal field is selected as $D/J = -1$. Our results are in good agreement with those plotted in Fig. 4.3(a). From Fig. 6.3(a), we can clearly see a peak at the critical temperature which corresponds to the divergence of the longitudinal susceptibility for $h/J = 0$. Furthermore, as it is seen from the figures, in the absence of a longitudinal magnetic field ($h/J = 0$), the curve of susceptibility rapidly increases and gives a peak at the phase transition temperature and then rapidly decreases as the temperature increases. In the presence of a longitudinal magnetic field, the phase transition is not observed, and the stronger the longitudinal magnetic field, the smaller is the susceptibility, reflecting the fact that the longitudinal magnetization is weaker. In Fig. 6.3(b), the longitudinal susceptibility is plotted in the absence of a longitudinal magnetic field with selected values of $D/J = 0, -0.5, -1, -1.5, -1.8$. We can clearly see from Fig. 6.3(b) that the critical temperature value k_BT_c/J

decreases as the absolute value of crystal field increases. From this point of view, this result is consistent with the results of Fig. 4.3(b). But the main difference between our effective-field theory analysis and Monte Carlo simulations appears at this point. While the critical temperature has been found to have a double valued form for $D/J < -1$ in our EFT study, there is no double-valued critical point appears for any value of crystal field D/J according to our MC simulations. This difference can be seen in detail from the phase diagrams of spin-1 system which are plotted by using both the EFT method and the MC simulation.

In Fig. 6.4, we show the influence of the longitudinal magnetic field on the internal energy and specific heat of the spin-1 BEG model. We can see that from Fig. 6.4(a), for the selected five values of h/J, if the longitudinal magnetic field increases, then the value of internal energy decreases. In the case of $h/J = 0$, the specific heat curve of spin-1 system in Fig. 6.4(b) exhibits a second order phase transition at the Curie temperature $k_BT/J = 1.41$ and rapidly decreases as the temperature increases. In the case of $h/J \neq 0$, there is no phase transition and, we see that the derivatives of internal energy are flattened with increasing external field. So, one can see that our EFT study and MC simulations are in good agreement at this point.

In the case of $h/J = 0$, we have plotted the temperature evolution of the internal energy U and specific heat C for spin-1 system on a square lattice at the selected values of D/J. The behavior of internal energy in terms of temperature and crystal field parameter is shown in figure Fig. 6.5(a) at fixed values of $D/J = -1.995, -1.5, -1, -0.5, 0$. The internal energy increases suddenly at the transition temperature as the crystal field parameter D/J gets just $D_t/J = -1.995$, which is similar to that in Fig. 4.5(a). But, note that in our EFT analysis we found the critical value of single-ion anisotropy as $D_t/J = -1.901$. For five selected values of the crystal field D/J, the specific heat C curves of the spin-1 system exhibit a second-order phase transition at the Curie temperature. As expected, the transition temperatures of C/Nk_B increase with the increasing crystal field strength (Fig. 6.5(b)). However, when D/J becomes $D/J \approx -1.9$, the discontinuity character of specific heat begins to increase in

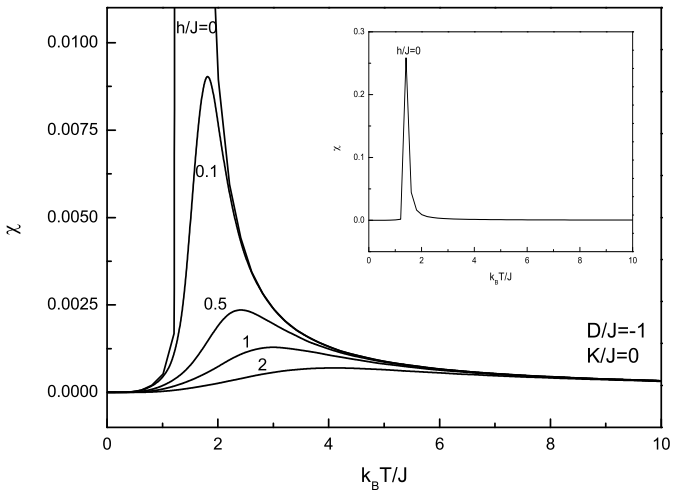

(a)

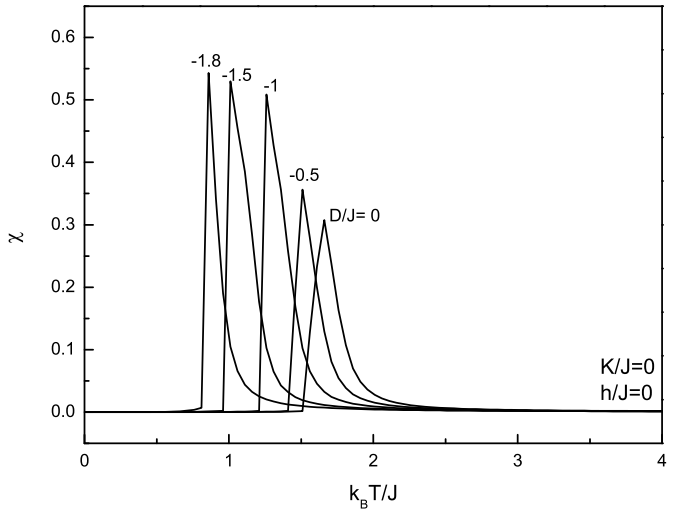

(b)

Figure 6.3 (a) The susceptibility for the spin-1 BEG model when the crystal field and biquadratic exchange interaction is selected as $D/J = -1$ and $K/J = 0$, respectively. The numbers on the each curve are the values of longitudinal magnetic field h/J. (b) The susceptibility for the spin-1 BEG model when the longitudinal magnetic field and biquadratic exchange interaction is selected as $h/J = 0$ and $K/J = 0$, respectively. The numbers on the each curve are the values of the crystal field D/J.

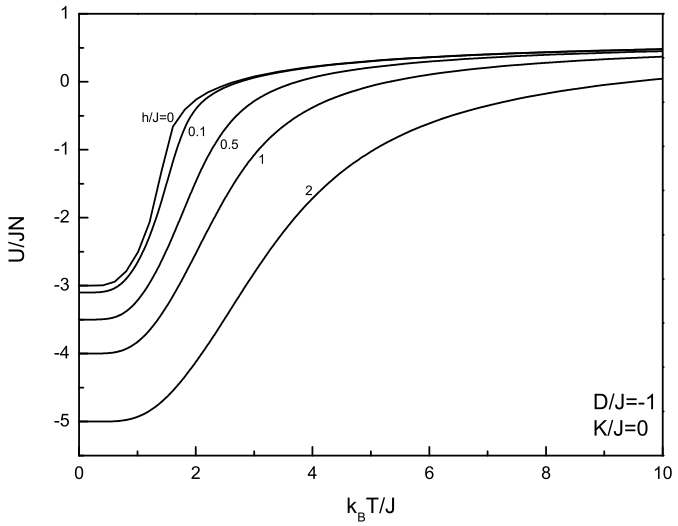

(a)

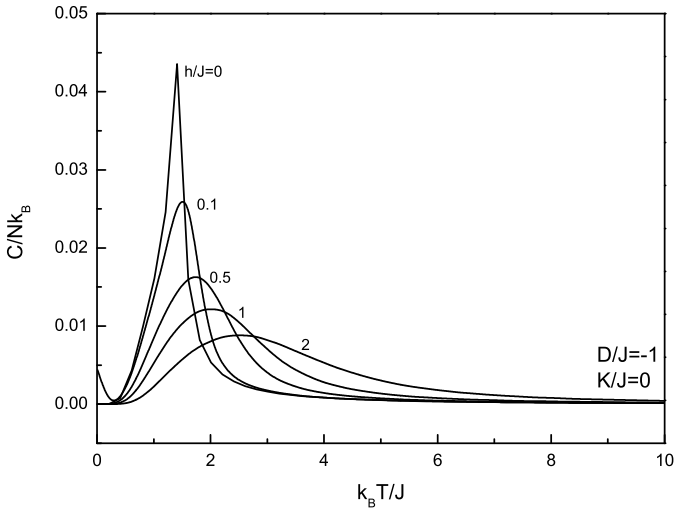

(b)

Figure 6.4 The temperature dependence of (a) the internal energy U and (b) the specific heat C for the spin-1 BEG model on a square lattice when the crystal field and biquadratic exchange interaction is selected as D/J=-1, $K/J = 0$, respectively at selected values of h/J= 0, 0.1, 0.5, 1 and 2.

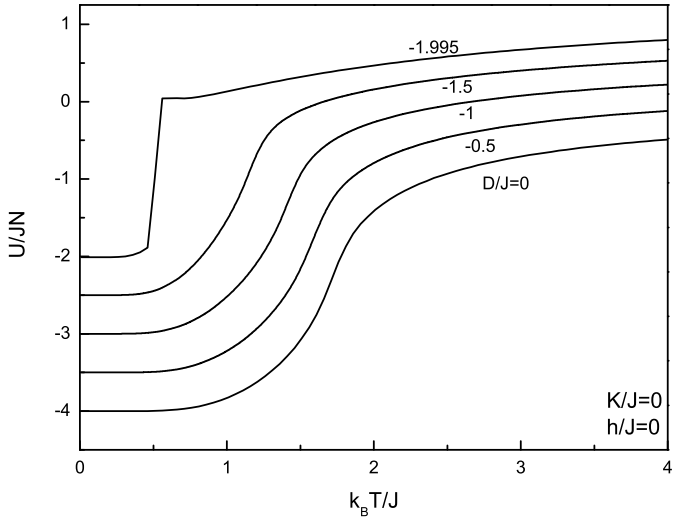

(a)

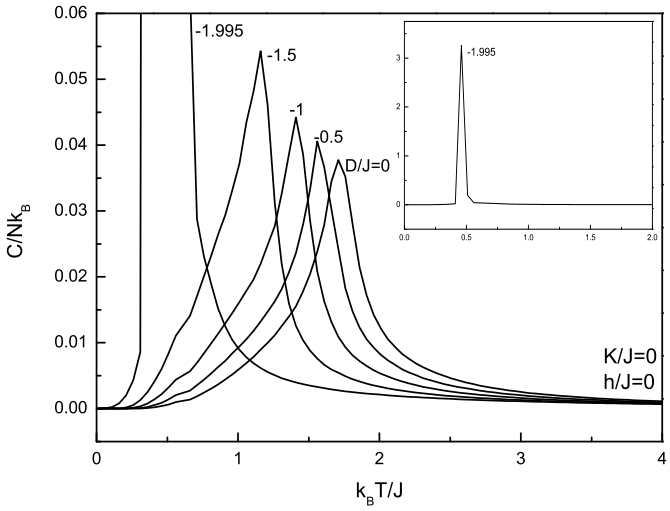

(b)

Figure 6.5 The temperature dependence of (a) the internal energy U and (b) the specific heat C for the spin-1 BEG model on a square lattice when the longitudinal magnetic field and biquadratic exchange interaction is selected as h/J=0, K/J = 0, respectively at selected values of D/J = -1.995, -1.5, -1, -0.5 and 0.

height. When the crystal field gets just to the value of its critical value $D_t/J = -1.995$, a jumping appears in the specific heat curve at the transition point and increases in height (as inset in the Fig. 6.5(b)). This behavior could be interpreted as a competition between the exchange interaction which tries to align the spins in the same direction, and the effect of the crystal field anisotropy which has the tendency to destroy this alignment in the considered system as discussed in previous section.

In order to investigate the influence of biquadratic exchange interaction K/J on the transition temperature k_BT_c/J, the longitudinal susceptibility is plotted in the absence of a crystal field ($D/J = 0$) and a longitudinal magnetic field ($h = 0$) with selected values of $K/J = 0, 0.5$ and 1. One can clearly see from Fig. 6.6 that the critical temperature value k_BT_c/J increases as the value of biquadratic exchange interaction increases and maximum point of each curve decreases as the value of biquadratic exchange interaction increases.

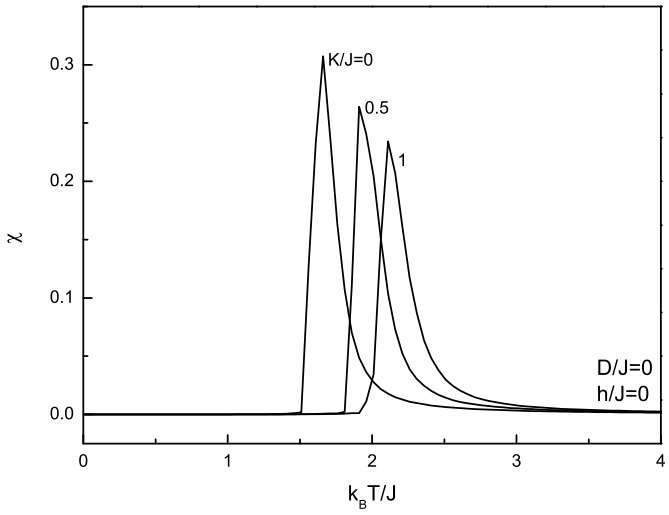

Figure 6.6 The susceptibility for the spin-1 BEG model when the crystal field and longitudinal magnetic field is selected as $D/J = 0$ and $h/J = 0$, respectively. The numbers on the each curve are the values of biquadratic exchange interaction K/J.

Next, in Fig. 6.7, in the case of $h/J \neq 0$, we have plotted the temperature dependencies of the longitudinal magnetization m and the susceptibility χ for the spin-1 BEG model on a square lattice at the selected values of K/J. We selected four typical biquadratic exchange interactions. As we can see from Fig. 6.7(a), when an external field is applied to the system, the absolute value of magnetization decreases slowly from its saturation magnetization value to the remaining magnetization value as the temperature increases and the remaining magnetizations are the same for all selected values of K/J at sufficiently large temperatures. Note that for $h/J \neq 0$, our results do not have a discontinuity behavior or phase transition point for any value of K/J and Fig. 6.7(a) and Fig. 6.7(b) curves have a continuous form and the absolute value of magnetization decreases more slowly as K/J increases.

Finally, in the case of $h/J \neq 0$, we show the influence of biquadratic exchange interaction K/J on the internal energy and the specific heat of the spin-1 BEG model on a square lattice for the selected values of K/J. As we can see from Fig. 6.8(a) and Fig. 6.8(b) our results do not have a discontinuity behavior or phase transition point for any value of K/J as in Fig. 6.7(a) and Fig. 6.7(b). Fig. 6.8(a) curves have a continuous form and the absolute value of internal energy increases as the selected values of K/J increases. It is seen from Fig. 6.8(b) that the specific heat curves have a relatively maximum-like Schottky peak at a certain value of the temperature and the height of the specific heat peak increases as the values of biquadratic exchange interaction increase up to $K/J = 1$, then starts to decreasing for the values of $K/J > 1$, and moves towards the increasing temperature when the biquadratic exchange interaction K/J increases. This behavior can be interpreted as a competition between the biquadratic exchange interaction K/J and the longitudinal external field h/J on the system. We also note that the Schottky-like round hump in the specific heat probably reflects the fact that the energy of the system depends not only on the longitudinal magnetic field h/J and the crystal field D/J, but also depends on the biquadratic exchange interaction K/J. Furthermore, as we discussed in previous section, they do not indicate that a second-order phase transition occurs in the 2D system and the shapes of the internal energy and specific heat curves obtained by

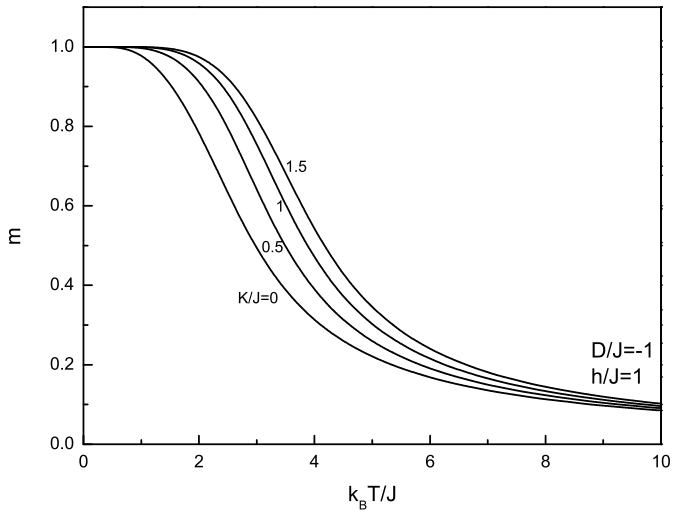

(a)

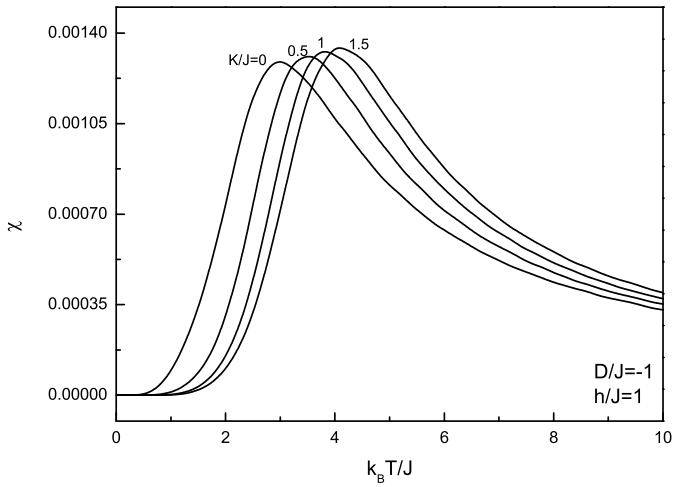

(b)

Figure 6.7 The temperature dependence of (a) the longitudinal magnetization m and (b) the susceptibility χ for the spin-1 BEG model on a square lattice when the crystal field and longitudinal magnetic field is selected as D/J=-1, $h/J = 1$, respectively, at selected values of $K/J = 0$, 0.5, 1, and 1.5. The numbers accompanying each line are the values of the biquadratic exchange interaction.

applied MC simulations qualitatively agree with those obtained by our EFT study. All calculated properties obtained by MC simulations also show the proper

thermodynamical behavior over the whole range of temperatures, including the ground state behavior ($\chi \to 0$ and $C \to 0$ for $T \to 0$) and the thermal stability condition ($C_h \geq 0$) as in our EFT results.

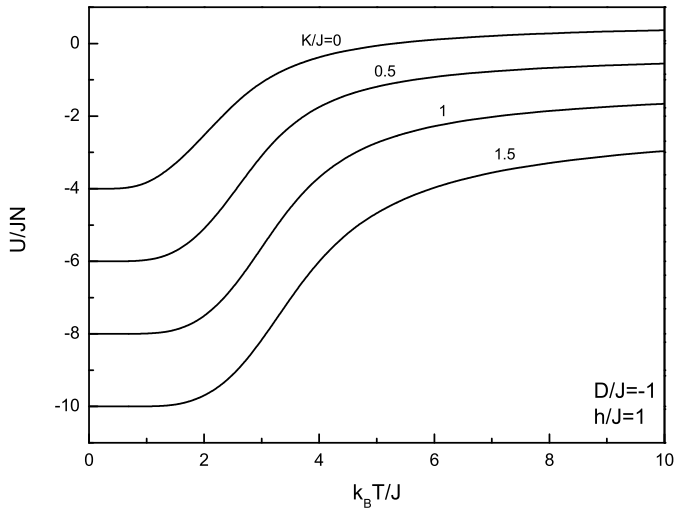

(a)

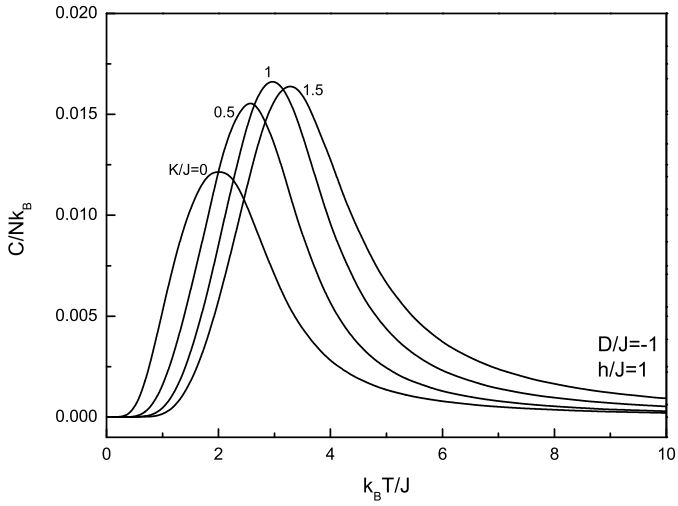

(b)

Figure 6.8 The temperature dependence of (a) the internal energy U and (b) the specific heat C for the spin-1 BEG model on a square lattice when the crystal field and longitudinal magnetic field is selected as D/J=-1, $h/J = 1$, respectively, at selected values of $K/J = 0$, 0.5, 1, and 1.5. The numbers accompanying each line are the values of the biquadratic exchange interaction.

CHAPTER SEVEN
PHASE DIAGRAM OF SPIN-1 ISING FERROMAGNETIC SYSTEM

7.1 Phase Diagrams for Spin-1 Blume-Capel Model

In this section, using EFT method and MC simulations, we have evaluated the phase diagrams of spin-1 Blume-Capel model and we have compared our MC simulation results and EFT analysis with other methods.

Firstly, the phase diagram of the spin-1 Ising system with single-ion anisotropy D/J and $q = 4$ is plotted in the $\left(\frac{k_B T_c}{J}, \frac{D}{J}\right)$ plane within the framework of effective field theory with correlations. In order to plot this curve, we assumed $\langle S_0 \rangle = \langle S_1 \rangle$, and the effective field γ is very small in the vicinity of $k_B T_c/J$ and solved the set of linear equations in equation (4.1.14) numerically using the self-consistent relation corresponding to equation (4.1.15).

Solid line in Fig. 7.1, shows the variation of the critical temperature $k_B T_c/J$ with crystal field D/J in the spin-1 Ising system with $q = 4$ and dashed line shows our MC simulation results. As mentioned in equation (4.2.1), for our EFT study, the critical temperature value at $D/J = 0$ is given as $k_B T_c/J = 1.964$. On the other hand, according to our MC simulations critical temperature value is given as $k_B T_c/J = 1.69$. Furthermore, the solid line on the plot shows that for $D/J < -1$, $k_B T_c/J$ becomes double valued. It implies that the spin-1 Ising system with $q = 4$ may exhibit a first order transition (or the tricritical behavior) below $D/J = -1$ at a negative tricritical value D_t/J. The value of critical D_t/J which is shown by white circle in Fig. 7.1 for $q = 4$ is equal to -1.901. The lower solution of the double-valued region between $D_t/J = -1.901$ and $D/J = -1$ just corresponds to the unstable solution and below the point $D_t/J = -1.901$, the $k_B T_c/J$ curve for spin-1 system does not have a physical meaning. But our MC simulations show that there is no double valued form of $k_B T_c/J$ for any value of D/J (dashed line in Fig. 7.1). At this point, one should notice that the solid lines

in Fig. 7.1 are clearly different from that (Du et al, 2003). Because the EBPA is a Bethe-Peierls-like approximation (Chakraborty, 1984) and the double-valued region does not appear in the k_BT_c/J curve of the spin-1 Ising system as in our MC simulations. In Table 7.1, we compare the values of D_t/J and k_BT_t/J at the tricritical point with those obtained by the other approximation methods. From Table 7.1, we see that the critical values of D_t/J and k_BT_t/J at the tricritical point obtained on a square lattice within the framework of our EFT method are much closer to the values obtained by EBPA (Du et al, 2003) than those obtained by the other approximation methods including our Monte Carlo simulations (MC) given in the same table.

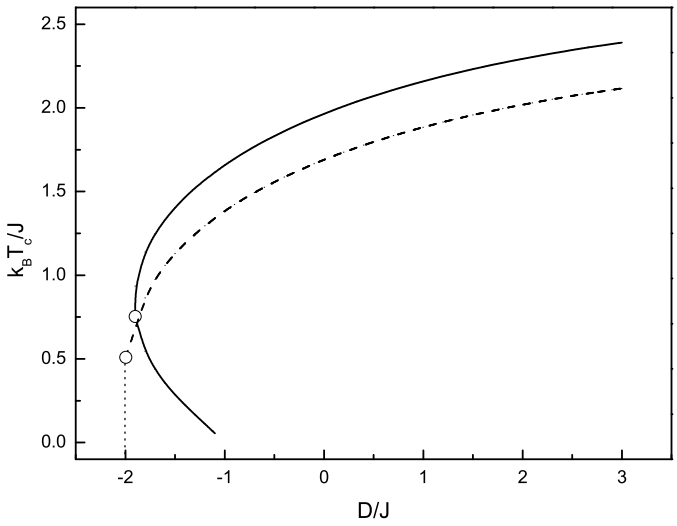

Figure 7.1 Phase diagram (k_BT_c/J versus D/J plot) of spin-1 Ising ferromagnetic system on square lattice ($q = 4$). The solid and dashed curves represent our results of EFT and Monte Carlo (MC) simulations, respectively. The white circles on each curve denote the tricritical points.

The critical single-ion anisotropy for the BC model is universally found to be $D_t/qJ = -0.47$ (Siqueira & Fittipaldi, 1986; Kaneyoshi et al, 1992b; Kaneyoshi, 1986). The phenomenon comes from the fact that the spin state at $T = 0K$ may change from the $S_i^z = \pm 1$ state to the $S_i^z = 0$ state at the critical value of $D/J = -q/2$. Our result of -0.475 with EFT on square lattice shows just a little

Table 7.1 Tricritical point D_t/J and the corresponding temperature k_BT_t/J obtained by several methods and the present work.

	MC	RG	EBPA	EFT	I-EFT
D_t/J	-1.995	-2.004	-1.906	-1.880	-1.901
k_BT_t/J	0.51	0.928	0.846	1.0	0.753

deflection from this value while -0.499 for MC is a little bit different from this value.

CHAPTER EIGHT
CONCLUSIONS

In this study we investigated the effects of crystal field, the longitudinal magnetic field, and the biquadratic exchange interaction on the magnetic properties of the spin-1 BC model and the spin-1 BEG model by using MC simulations and the introduced EFT approximation and also compared the phase diagrams obtained by using MC simulation and the introduced EFT method for the BC model. Using the introduced EFT method, we can easily obtain multi-spin correlation functions without any kind of decoupling approximation, so it was found that the critical temperature for BC model is much closer to those obtained by the expanded Bethe-Peierls and Bethe approximation than those obtained by MFA, SE, EFT and DA approximations. On the other hand, according to our MC simulations, the critical temperature value of the BC model with $q = 4$ is in a good agreement with those of series expansion method.

Furthermore, we have discussed in detail the influence of longitudinal magnetic field, crystal field and biquadratic exchange interaction on the magnetizations, susceptibilities, internal energies and the specific heats of the BC model and the BEG model, respectively. Using MC simulation method, we found that the type of the hysteresis loops does not depend on the biquadratic exchange interaction.

In the previous sections, we have shown and discussed some typical results for spin-1 system on the square lattice. On the basis of our analysis, we can conclude that the introduced EFT method which considered partially the spin-spin correlations has been successfully applied to a kind of Ising spin problem, which is superior to conventional mean field theory and the EFT theory in the literature.

The phase diagrams of the BC model has been studied by different techniques in the literature: Using the mean field approximation, effecetive-field theory, Bethe approximation, series expansion methods, renormalization group theory, finite cluster approximation, constant-coupling approximation and the cluster-

variational method. Most of these approximate schemes predict in the BC model the existence of a tricritical point at which the phase transition changes from second-order to first-order when the value of D becomes sufficiently negative. Our results show that the tricritical point value obtained by MC simulations is much closer to those of Renormalization group method, on the other hand, the value of D_t/J obtained by introduced EFT approximation is much closer to the result of expanded Bethe-Peierls method.

In contrast to the results of MC simulations (dashed line in Fig. 7.1), within the framework of our introduced EFT method (solid line in Fig. 7.1), we found that for $D/J < -1$, k_BT_c/J becomes double valued. It implies that the spin-1 Ising system with $q = 4$ may exhibit a first order transition (or the tricritical behavior) below $D/J = -1$ at a negative tricritical value D_t/J. The lower solution of the double-valued region between $D_t/J = -1.901$ and $D/J = -1$ just corresponds to the unstable solution and below the point $D_t/J = -1.901$, the k_BT_c/J curve for spin-1 system does not have a physical meaning. Furthermore, the critical single-ion anisotropy for the BC model is universally found to be $D_t/qJ = -0.47$. Our result of -0.475 with introduced EFT on square lattice shows just a little deflection from this value while -0.499 for MC is a little bit different from this value.

We hope that our results will be potentially very useful for studying and understanding more complicated Ising ferromagnetic systems in the presence of the biquadratic exchange interaction, the crystal field, and longitudinal magnetic field.

REFERENCES

Adler, J., & Enting, I. G. (1984). The two-dimensional spin-1 Ising system and related models. *J. Phys. A*, *17* (11), 2233-2245.

Balcerzak, T. (2002). On the exact identities for Ising model with arbitrary spin. *J. Magn. Magn. Mater.*, *246*, 213-222.

Balcerzak, T. (2003). Thermodynamics of the Ising model in pair approximation. *Physica A*, *317* (1-2), 213-222.

Baxter, R. J. (1982). Exactly Solved Models in Statistical Mechanics. Academic Press, Newyork.

Berlin, T. H. & Kac, M. (1952). The Spherical Model of a Ferromagnet. *Phys. Rev.*, *86* (6), 821-835.

Bethe, H. A. (1935). Statistical theory of superlattices. *Proc. R. Soc. London Ser. A*, *150*, 552-575.

Binder, K. (1981). Critical Properties from Monte Carlo Coarse Graining and Renormalization. *Phys. Rev. Lett.*, *47* (9), 693-696.

Blote, H. W. J., & Nightingale, M. P. (1985). Universality in two-dimensional Ising models. *Physica A*, *134* (1), 274-282.

Blume, M. (1966). Theory of the First-Order Magnetic Phase Change in UO_2. *Phys. Rev.*, *141* (2), 517-524.

Blume, H., Emery V. J., & Griffiths, R. B. (1971). Ising model for the λ transition and phase separation in ^{3}He $-^4$ He mixtures. *Phys. Rev. A*, *4* (3), 1071-1077.

Bobak, A. & Jurcisin, M. (1997). A discussion of critical behaviour in a mixed-spin Ising model . *Physica A*, *240*, 647-656.

Boccara, N. (1983). Dilute Ising model: a simply theory. *Phys. Lett. A*, *94*, 185.

Bocarra, N. & Benyoussef, A. (1983). Phase diagrams of random Ising models: simple and systematic successive approximation. *J. Phys. (France)*, *4*, 1143-1147.

Callen, H. B. (1963). A note on Green functions and the Ising model. *Phys. Lett.*, *4*, 161.

Canpolat, Y., Torgürsül, A., & Polat, H. (2007). The magnetic properties of spin-1/2 ans spin-1 Ising models in an applied magnetic field by introducing the effective-field approximation. *Phys. Scr.*, *76* (6), 597-605.

Capel, H. (1966). On the possibility of first-order phase transitions in Ising systems of triplet ions with zero-field splitting. *Physica (Amsterdam)*, *32* (5), 966-988.

Chakraborty, K. G. (1984). Statistical mechanics of a Bethe lattice. *Z. Phys. B; Condens. Matter*, *55*, 231-234.

Du, A., Yü, Y. Q. & Liu, H. J. (2003). Expanded Bethe-Peierls approximation for the Blume-Capel model. *Physica A*, *320*, 387-397.

Du, A., Liu, H. J. & Yü, Y. Q. (2004). Expanded Bethe-Peierls approximation for the Ising model with S=1/2 and 1. *Phys. Stat. Sol. (B)*, *241* (1), 175-182.

Ekiz, C. (2005). Ferrimagnetism in the mixed spin Ising system on a two-fold Cayley tree. *J. Magn. Magn. Mater.*, *293* (2), 759-767.

Ekiz, C. & Keskin, M. (2003). Magnetic properties of the mixed spin-1/2 and spin-1 Ising ferromagnetic system. *Physica A*, *317* (3-4), 517-534.

Fox, P. F., & Guttman, A. J. (1985). Low temperature critical behaviour of the Ising model with spin $S > 1/2$. *J. Phys. C*, *6* (5), 913-932.

Gould, H. & Tobochnik J. (1996). *An Introduction to Computer Simulation Methods. Applications To Physical Systems* (2nd Edition). Addison-Wesley Publishing Company.

Honmura, R. (1984). Correlated-effective-field treatment of the anisotropic Ising ferromagnet: Thermodynamical properties. *Phys. Rev. B*, *30* (1), 348-358.

Honmura, R., & Kaneyoshi, T. (1979). Contribution to the new type of effective-field theory of the Ising model. *J. Phys. C*, *12* (19), 3979-3992.

Htoutou, K., Benaboud, A., Ainane, A., & Saber, M. (2004). The phase diagrams and the order parameters of the transverse spin-1 Ising model with a longitudinal crystal-field. *Physica A*, *338* (3-4), 479-492, and references therein.

Jiang, W., & Bai, B. D. (2005). Magnetic properties of a spin system in a longitudinal magnetic field. *J. Appl. Phys.*, *97* (10), 10B307.

Jiang, W., & Bai, B. D. (2006). Hysteresis loops and susceptibility of ferromagnetic or ferrimagnetic bilayer system. *Phys. Stat. Sol. (B)*, *243* (12), 2892-2900.

Jiang, W., Bai, B. D., & Wei, G. Z. (2005). Magnetic properties of biaxial spin systems in a longitudinal magnetic field. *Physica A*, *354*, 301-311.

Jiang, W., Guo, L. Q., Wei, G. Z., & Du, A. (2001). Longitudinal and transverse magnetizations of spin-3/2 transverse Ising model with the crystal field on square lattice. *Physica B*, *307*, 15-21.

Jiang, W., & Wei, G. Z. (2000). Properties of spin-3/2 transverse Ising model with anisotropic crystal field on a honeycomb lattice. *Physica A*, *284* (1-4), 215-222.

Jiang, W., & Wei, G. Z., & Xin, Z. H. (2000). Effect of a crystal field on phase transitions in a spin-3/2 transverse Ising model. *J. Magn. Magn. Mater.*, *217* (1-3), 225-230.

Jiang, W., & Wei, G. Z., & Xin, Z. H. (2000). Phase diagrams and tricritical behavior of spin-2 Ising model with a transverse crystal field. *Phys. Stat. Sol. (B)*, *221* (2), 759-765.

Kaneyoshi, T. (1980). Comments on molecular-field theory with correlations. *Phys. Lett.*, *76* (1), 67-68.

Kaneyoshi, T. (1986). The tricritical point in Ising models with random bonds and crystal-field interactions. *J. Phys. C*, *19* (25), L557-L561.

Kaneyoshi, T. (1987). Curie Temperatures and Tricritical Points in Mixed Ising Ferromagnetic Systems. *J. Phys. Soc. Japan*, *56*, 2675-2680.

Kaneyoshi, T. (1988). Phase transition of the mixed spin system with a random crystal field. *Physica A*, *153* (3), 556-566.

Kaneyoshi, T. (1992). Differential operator technique in the Ising spin systems. *Acta. Phys. Pol. A*, *83*, 703-738.

Kaneyoshi, T. (1999). A new type of cluster theory in Ising models (I). *Physica A*, *269*, 344-356.

Kaneyoshi, T. (1999). A new type of cluster theory in Ising models (II). *Physica A*, *269*, 357-368.

Kaneyoshi, T. (2000). Decoupling approximation in spin-S ($S \geq 1/2$) Ising systems. *Physica A*, *286* (3-4), 518-530.

Kaneyoshi, T., Fittipaldi, I. P., Honmura, R. &Manabe, T. (1981). New correlated-effective-field theory in the Ising model. *Phys. Rev. B*, *24* (1), 481-484.

Kaneyoshi, T., Jascur, M. (1992). Specific heat of the spin-3/2 Blume-Capel model. *Phys. Rev. B*, *46* (6), 3374-3379.

Kaneyoshi, T., Jascur, M., &Tomczak, P. (1992a). The ferrimagnetic mixed spin-1/2 and spin-3/2 Ising system. *J. Phys.: Condens. Matter*, *4* (49), L653-L658.

Kaneyoshi, T. & Tamura, I. (1982). Statistical mechanics of anisotropic two-dimensional Ising systems; application of new correlated effective-field theory. *Phys. Rev. B*, *25* (7), 4679-4684.

Kaneyoshi, T., Tucker J. W., Jascur, M. (1992b). Differential operator technique for higher spin problems. *Physica A*, *186* (3-4), 495-512.

Landau, D. P. & Binder, K. (1996). *A Guide to Monte Carlo Simulations in Statistical Physics*. (2nd Edition). Cambridge University Press.

Lines, M. E. (1974). Correlated-effective-field theory: A statistical approach for grossly anharmonic lattice vibrations. *Phys. Rev. B*, *9* (3), 950-957.

Mancini, F., & Naddeo, A. (2006). Equations-of-motion approach to the spin-1/2 Ising model on the Bethe lattice. *Phys. Rev. E*, *74*, 061108.

Matsudaira, N. (1973). Ising ferromagnets with random impurities. *J. Phys. Soc. Jpn.*, *35*, 1593-1599.

Micnas, R. (1979). Application of the functional integral method to the classical and quantum spin models. *Physica A*, *98* (3), 403-441.

Mielnicki, J., Balcerzak, T., Truong, V. H., Wiatrowski, G., & Wojtczak, L. (1986). A simple method of basic properties description of diluted ferromagnetic alloys (Ising model, S=1/2). *J. Magn. Magn. Mater.*, *58* (3-4), 325-333.

Ng, W. M., & Barry, J. H. (1978). Cluster-variation method applied in the pair approximation to the S=1 Ising ferromagnet having additional single-ion-type uniaxial anisotropy. *Phys. Rev. B*, *17* (9), 3675-3683.

Onsager, L. (1936). Electric moments of molecules in liquids. *J. Am. Chem. Soc.*, *58*, 1486.

Onsager, L. (1944). Crystal statistics I. a two dimensional model with an order-disorder transition. *Phys. Rev.*, *65* (3-4), 117-149.

Pawley, G. S., Sweden, R. H., Wallace, D. J., & Wilson, K. G. (1984). Monte Carlo renormalization-group calculations of critical behavior in the simple-cubic Ising model. *Phys. Rev. B*, *29* (7), 4030-4040.

Peierls, R., (1936). On Ising's model of ferromagnetism. *Proc. Cambridge Philos. Soc. B*, *32*, 477.

Polat, H., Akıncı, Ü., & Sökmen, İ. (2003). A method for phase diagrams of spin-1 Ising ferromagnetic systems. *Phys. Stat. Sol. (B)*, *240* (1), 189-200.

Rachadi, A., & Benyoussef, A. (2004). Monte Carlo study of the Blume-Emery-Griffiths model at the ferromagnetic-antiquadrupolar-disordered phase interface. *Phys. Rev. B*, *69* (6), 064423.

Saul, D. M., Wortis, M., & Stauffer, D. (1974). Tricritical behavior of the Blume-Capel model. *Phys. Rev. B*, *9* (11), 4964-4980.

Siqueira, A. F. & Fittipaldi, I. P. (1986). New effective-field theory for the Blume-Capel model. *Physica A*, *138* (3), 592-611.

Suzuki, M. (1965). Generalized exact formula for the correlations of the Ising model and other classical systems. *Phys. Lett.*, *19* (4), 267-268.

Tamura, I. & Kaneyoshi, T. (1981). Ising ferromagnets with random anisotropy. *Prog. Theor. Phys.*, *66*, 1892-1894.

Tanaka, Y. & Uryu, N. (1981). A new method for calculation of the magnetic properties in one-dimensional and two-dimensional spin systems with anisotropic Heisenberg exchange. *J. Phys. Soc. Jpn.*, *50*, 1140.

Wei, G. Z., Liang, Y. Q., Zhang, Q., & Xin, Z. H. (2004). Magnetic properties of mixed-spin Ising systems in a longitudinal magnetic field. *J. Magn. Magn. Mater.*, *271* (2-3), 246-253.

Yeomans, J. M. (2000). *Statistical Mechanics of Phase Transitions* (5th Edition). Clarendon Press Oxford.

Yokota, T. (1988). Double-chain approximation for the Ising model. *Phys. Rev. B*, *38* (1), 638-640.

Zernike, F. (1940). The propagation of order in co-operative phenomena : Part I. The AB case. *Physica*, *7* (7), 565-585.

APPENDIX

Within the framework of the effective-field theory, the Hamiltonian corresponding to the BC model can be separated into two parts: one (denoted by H_i) includes all parts of H associated with the site i, and the other (denoted by, $H^{'}$) does not depend on the site i. Then, $H = H_i + H^{'}$, where $-H_i$ is given by

$$-H_i = E_i S_i^z + D\left(S_i^z\right)^2 + hS_i^z$$

with

$$E_i = J\sum_j S_j^z$$

In order to derive the formulation of the function $F(x)$, we need the matrix representation of the spin operator S_i^z and it is given by,

$$S_i^z = \begin{pmatrix} 1 & 0 & 0 \\ 0 & 0 & 0 \\ 0 & 0 & 1 \end{pmatrix}$$

and in S_i^z representation, $-H_i$ can be rewritten in the form of a 3×3 matrix as

$$-H_i = \begin{pmatrix} E_i + D + h & 0 & 0 \\ 0 & 0 & 0 \\ 0 & 0 & -E_i + D - h \end{pmatrix}$$

The general form of the function $F(x)$ is defined by, (Jiang et al, 2005)

$$F(x) = \frac{1}{\sum_{n=1}^{3}\exp(\beta\lambda_n)}\left\{\sum_{n=1}^{3}\langle\varphi_n|S_i^z|\varphi_n\rangle\exp(\beta\lambda_n)\right\} \tag{A.1}$$

here, λ_n $(n = 1, 2, 3)$ is eigenvalue and $|\varphi_n\rangle$ represents eigenvector with the eigenvalue λ_n of $-H_i$. Eigenvalues and corresponding eigenvectors of $-H_i$ can be easily found as

$$\lambda_1 = 0 \qquad \varphi_1 = \begin{pmatrix} 0 \\ 1 \\ 0 \end{pmatrix}$$

$$\lambda_2 = -E_i + D - h \qquad \varphi_2 = \begin{pmatrix} 0 \\ 0 \\ 1 \end{pmatrix}$$

$$\lambda_3 = E_i + D + h \qquad \varphi_3 = \begin{pmatrix} 1 \\ 0 \\ 0 \end{pmatrix}$$

If we insert this relations into (A.1), we obtain the desired relation

$$F(x) = \frac{2\sinh[\beta(E_i + h)]}{2\cosh[\beta(E_i + h)] + \exp(-\beta D)} \tag{A.2}$$

Note that, when $D \to \infty$, the function $F(x)$ reduces to $\tanh(\beta x)$ and hence (A.2) becomes equivalent to (3.1.10). In other words, when D takes a large positive value, the BC model behaves like the standard spin-1/2 Ising model and in this case the $S_i^z = 0$ state is not allowed energetically.

In order to derive the definition of the function $G(x)$, one has to introduce the relation (Jiang et al, 2005)

$$G(x) = \frac{1}{\sum_{n=1}^{3} \exp(\beta\lambda_n)} \left\{ \sum_{n=1}^{3} \langle\varphi_n|(S_i^z)^2|\varphi_n\rangle \exp(\beta\lambda_n) \right\} \tag{A.3}$$

Following the same procedure as in derivation of the function $F(x)$, we can easily obtain the relation corresponding to $G(x)$ by substituting the eigenvalues and the

corresponding eigenvectors of $-H_i$ into definition (A.3)

$$G(x) = \frac{2\cosh[\beta(E_i + h)]}{2\cosh[\beta(E_i + h)] + \exp(-\beta D)} \tag{A.4}$$